Thermal Front Velocity Modelling and Lumped Parameter Simulation

Yapi Donatien Achou

Thesis of 30 ECTS credits
Master of Science (M.Sc.) in Sustainable Energy Engineering

June 2016

Thermal Front Velocity Modelling and Lumped Parameter Simulation

Thesis of 30 ECTS credits submitted to the School of Science and Engineering
at Reykjavík University in partial fulfillment of
the requirements for the degree of
Master of Science (M.Sc.) in Sustainable Energy Engineering

June 2016

Supervisor:

Dr. Guðni Axelsson, Supervisor
, Iceland Geosurvey, Iceland

Dr. Ágúst Valfells, Co-advisor
, Reykjavík University, Iceland

Examiner:

Sæunn Halldórsdóttir, Examiner
Department head, Earth science, Iceland Geosurvey, Iceland

Thermal Front Velocity Modelling and Lumped Parameter Simulation

Yapi Donatien Achou

June 2016

Abstract

Geothermal reservoir engineering provides various methods to study, analyse and predict the behaviour of a geothermal system. In this thesis, we use two, cost and time effective methods to study a low temperature geothermal system located in Munadarnes situated in west Iceland. By using these two models, we derive important properties of a geothermal reservoir in Munadanes. Reinjection is studied and used to improve the production potential of the reservoir. Injection of cold fluid into hot geothermal reservoirs is formulated as conservation laws. The cold front velocity induced during injection has been computed from the literature from conservation of energy and the method of characteristics applied to an initial boundary value problem. This computed thermal front velocity is expressed as the ratio of the integral of the product of the internal energy and the energy flux to the integral of the internal energy. In this thesis we present a new and innovative method for computing the thermal front velocity by solving a Riemann problem. We show that the unique solution of the Riemann problem moves at the speed equal to the thermal front velocity. The thermal front velocity computed in this thesis is only expressed as the integral of the energy flux. Our result is computed from the Rankine-Hugoniot shock condition from the theory of hyperbolic conservation laws and is much easier to evaluate. It depends on the flux function of the conservation laws, the injected fluid temperature and the reservoir temperature. A relative error of magnitude 10^{-3} was observed between the result obtained in this thesis and the one from the literature. This shows that the two results are in good agreement. By Applying lumped parameter modelling to well $MN08$ in Munadanes in west Iceland, the size of the reservoir, base on an estimated 900 m reservoir depth, the permeability and the storage mechanism of the reservoir intersecting well $MN08$ are evaluated. Diverse injection scenarios are used to determine the optimum distance separating injection well and production well in Munadanes, in order to mitigate temperature drop due to cold water injection. The models used to compute the thermal front velocity assume that 100% of the injected fluid reaches the production well. In reality only a fraction of the injected fluid reaches the production well. For practical reinjection field study, a tracer test is recommended. In addition, the models are one dimension and could be extended to 2 or 3 dimensions.

Titll verkefnis

Yapi Donatien Achou

júní 2016

Útdráttur

Thermal Front Velocity Modelling and Lumped Parameter Simulation

Yapi Donatien Achou

Thesis of 30 ECTS credits submitted to the School of Science and Engineering
at Reykjavík University in partial fulfillment of
the requirements for the degree of
Master of Science (M.Sc.) in Sustainable Energy Engineering

June 2016

Student:

.....

Yapi Donatien Achou

Supervisor:

.....

Dr. Guðni Axelsson

.....

Dr. Ágúst Valfells

Examiner:

.....

Sæunn Halldórsdóttir

.....
date

.....
Yapi Donatien Achou
Master of Science

Acknowledgements

This Masters's thesis was worked on during a challenging period of my life. The present work would not have been possible without my supervisors Guðni Axelsson and Ágúst Valfells, to whom I would like to say special thank you. I greately appreciate the generosity which Guðni Axelsson showed me with regards to his availability, time and guidance. I also thank all the faculties and staff at Iceland School of Energy and Reykjavik University who gave me the opportunity to complete this work. I am also grateful to professor Robert Magnus from the University of Iceland for his help. I would like to say special thank you to Reykjavik Energy for their support and permission to use data from Munadarnes.

Yapi Donatien Achou

Contents

List of Figures

List of Tables

List of Symbols

Symbol	Description	Value/Units
ϕ	Prosity	no unit
V_{total}	Total rock volume	m^3
V_P	Pore volume	m^3
V_S	Solid volume	m^3
Q	Fluid flow rate	$kgs^{-1}m^{-2}$)
K	Permeability tensor	matrix
K_x, K_y, K_z	x, y, z components of permeability tensor	
ρ	Density	Kgm^{-3}
ν	Kinematic viscosity	m^2s^{-1}
∇P	Pressure gradient	Pa/m
g	Acceleration due to gravity	9.81 ms^{-2}
V_{ca}	Characteristic velocity in Reynolds number	ms^{-1}
d_{ca}	Characteristic flow path diameter in Reynolds number	m
R_e	Reynolds number	Dimensionless
v_p	Pore velocity or interstitial velocity	$kgs^{-1}m^{-2}$
V_c	Volume of cold water	m^3
V_h	Volume of hot water	m^3
β	Fluid compressibility	Pa^{-1}
α	Expansivity	K^{-1}
P	Pressure	$Kgm^{-1}s^{-2}$
m	Mass	Kg
$\mathbf{q}_f$	Heat flux density from Fourier's law of heat conduction	Wm^{-2}
λ	Thermal conductivity	$Wm^{-1}K^{-1}$
∇T	Temperature gadient	K
S_l	Liquid saturation	
S_g	gas saturation	
f_l	Gas concentration of chemical species in liquid	Kgm^{-3}
f_g	Mass concentration of chemical species in gas	Kgm^{-3}
q_m	Mass sink source	Kg
u_l	Liquid velocity	ms^{-1}
u_g	Gas velocity	ms^{-1}
∇	gradient operator	
U	Internal energy	m^2Kgs^{-1}
U_r	Internal energy of rock	m^2Kgs^{-1}
U_g	Internal energy of gas	m^2Kgs^{-1}
q_E	Energy sink source	Jm^3s^{-1}
T	Temperature	K unless specified
k	Absolute permeability	Darcy
P_l	Liquid pressure	$Kgm^{-1}s^{-2}$
P_g	Gas pressure	$Kgm^{-1}s^{-2}$
k_{rl}	Relative permeability of the rock to liquid	Darcy
k_{rg}	Relative permeability of the rock to gas	Darcy
z	z axis	

Chapter 1

Introduction

With an increasing world population, energy consumption is directly linked to the survival of the human species. With three quarters of the world energy source coming from fossil fuel in 2004 [13], the world is subjected to an environmental crisis linked to our energy sources. The need for clean and renewable energy has never been that important as it is today. Geothermal energy is classified as clean and renewable energy that has the potential of contributing significantly to sustainable energy use in many parts of the world [10]. Mainly generated by radioactive elements in the crust and mantle of the earth, geothermal energy provides theoretically almost an unlimited source of energy for the world population.

Geothermal energy production at a sustainable rate has been defined as production that can be maintained for $100-300$ years [10, 3]. This requires knowledge and understanding of the geothermal system, sustainable production schemes such as reinjection of energy depleted water and good management strategies. These strategies involve a multidisciplinary field of studies comprising geology, geophysics, chemistry and mathematics. Through geological exploration, a deeper insight into the viability of a geothermal project is provided. The geological survey can for example reveal thermal and hydrological activities at depth in the earth crust. Geophysical methods provide a mean to assess and quantify physical properties of the geothermal systems. They can reveal the location of fracture zones, the tectonic features of the geothermal reservoir and even provide information on temperature distribution of the entire geothermal field. The chemical content of the geothermal fluid can be an indicator of reservoir temperature and can explain temperature fluctuations within the reservoir boundary. Chemical analysis of the fluid can for example help predict and prevent surface equipment and pipe corrosion. With the development of modern computer architectures, numerical simulation combined with geological, geophysical and chemical data, plays a key role in geothermal resource management. It allows detail modelling of an entire geothermal system. However, numerical simulation requires a large amount of data for model calibration. It is time consuming and expensive. Cost and time effective, powerful alternatives to detail numerical simulation are analytical methods. Through analytical solutions of differential equations, physical conditions or properties of the reservoir can be approximated. Analytical methods require less amount of data than numerical simulation and are regularly used in geothermal reservoir engineering. This includes reinjection research.

Many pioneering works have been performed or publish in the field of geothermal engineering. Axelsson, Barker and Stefansson presented reinjection of water as a resource management strategy [10, 7, 2, 11, 50]. Bodvarsson was the first to derive an analytical method for calculating the thermal front velocity induced during injection of cold water in a hot

geothermal reservoir for constant rock and fluid properties [17]. His method was later extended for temperature independent rock and fluid properties [48]. A method for analysing tracer test data used in reinjection was derived by Axelsson et al. [7]. A lumped parameter modelling technique was developed by Axelsson to simulate pressure response due to production in a low temperature geothermal system [6, 5]. Bjornsson developed the well bore simulator HOLA capable of simulating steady state two phase flow in a multi feed zones geothermal well [15].

One major issue with renewable energy such as geothermal energy, is efficiency. In order for geothermal energy to be competitive on the global energy market, its efficiency need to increase significantly. The objective of this thesis is to present and test two cost and time effective modelling methods used in geothermal engineering and applied to low temperature geothermal systems. These modelling methods include the thermal front velocity induced by injection of energy depleted water into a hot geothermal reservoir, and lumped parameter modelling. The two methods are later tested on the Munadarnes geothermal system located in west Iceland. In this thesis reinjection is presented as an essential part of sustainable production of geothermal energy.

The contribution of this thesis can be outline as followed: By using an analytical solution of water flow in a one dimension channel, the cooling response of the production well due to injection of cold water is presented. Cooling is minimised by placing the reinjection well at a few km from the production well. The rate at which the injected cold front advances is computed by using the theory of hyperbolic conservation laws. The result obtained is compared with the one in the literature with signifficant agreement. The lumped parameter modelling method is applied to the Munadarnes low temperature geothermal reservoir located in west Iceland. The simulation reveals that the reservoir permeability is high. Multiple reinjection scenarios with different production and reinjection rates show that reinjection increases significantly the pressure of the reservoir.

The thesis is organised as follows: In Chapter 2 the thermal and hydrological properties of hydrothermal systems are presented. The Chapter ends with a brief presentation of geothermal resource assessment methods including reinjection schemes. Chapter 3 presents the derivation of the thermal front velocities from three approaches. The chapter starts by presenting the general mathematical equation, followed by the early approach. The recent approach is then outlined followed by the new approach which is one of the contribution of this thesis. The Chapter ends by comparing the three approaches while emphasising the limitation of the mathematical models. In Chapter 4 the theoretical background of lumped parameter modelling are presented. Chapter 5 presents a case study: The thermal front velocities computed in Chapter 3 are applied to the Munadarnes low temperature geothermal system located in west Iceland. The corresponding arrival times of the injected cold water are computed for different scenarios. By using a one dimensional channel model, the temperature profile of the system, under injection of cold water is computed. The lumped parameter modelling is then applied to the Munadarnes system to compute the pressure response with and without injection. The size, permeability and storage mechanism of the Munadarnes geothermal system are derived from lumped parameter simulation. Chapter 6 present the conclusion and recommendation on future work.

Chapter 2

Background

2.1 Hydrothermal system

Hydrothermal systems can be defined as underground systems with a set of processes that redistribute energy and mass in response to fluid circulation [39]. Hydrothermal systems include heat, fluid and sufficient permeability in the natural geological formation. In hydrothermal systems such as geothermal systems, the heat source depends on the type of system. On one side we have the volcanic systems heated by magma chambers and hot intrusions, and on the other side we have the normal crust heated to a large extend by radioactive elements such as potassium 40, thorium 232, and uranium 235 and 230. In-between these we have different types of systems with different heating mechanism. For example sedimentary systems are mostly heated by the earth normal heat flow, while systems controlled by fractures are heated by heat from the crust, which is remnant heat from volcanism and to a much smaller extend radioactivity.

2.1.1 Hydrological properties

One of the main hydrological properties is porosity, as hydrothermal systems are mainly an interconnection of fractures. However, a hydrothermal system can be approximated by porous medium in the hydrological sense. A porous medium contains voids or pores, allowing fluid to be trapped or to flow throughout the medium. In the context of geothermal energy, we are interested in the voids within the subsurface geological formation such as rock. To allow fluid flow, the pore spaces must form a network of interconnected voids space. Based on the time they were formed, the pores space can be divided in two [12]. Original pore spaces are formed during the rock formation, while secondary pore spaces are formed after the rock formation [12]. Secondary porosity is due to physical and chemical changes occurring during the conversion of one rock type to an other, or due to tectonic activity [12]. Porous media can be classified based on their constituents: Intragranular porous media created by voids within the rock grains and intergranular porous media formed by the voids between the rock grains [12]. Fracture porosity is due to fractures within the rock caused by tectonic forces. On the basis of mechanical properties, we can distinguish between consolidated porosity and unconsolidated porosity [12]. In the consolidated case, the grains are kept together with a cementing material, while in the unconsolidated case the grains are loose [12].
Porosity ϕ, is a statistical measure of the void spaces with respect to the total rock volume and can be expressed as

$$\phi = \frac{V_P}{V_{total}} = 1 - \frac{V_S}{V_{total}}$$

where

$$V_{total} = V_S + V_P$$

is the total rock volume, while V_P and V_S are the pore volume and solid (rock) volume, respectively. Figure 2.1 shows a porous medium with a connected network of pores. In geothermal systems, only effective porosity is of importance, because it reflects interconnected pores and allows fluid to flow. Effective porosity affects the storage capacity of the medium, which is its ability to absorb or release fluid in response to pressure change, due to fluid extraction or fluid injection in the medium. Alternatively, we can define fracture porosity as the fraction of volume occupied by fractures. The recharge mechanism of porous medium are partly due to precipitation from the highlands, that infiltrate the ground under gravity, filling up the interconnected pores space to form a saturation zone, [12]. When a part of the porous medium is trapped between impermeable formations, it is termed confined. Alternatively, an unconfined aquifer is bounded above by a water table. The movement of isothermal water in porous medium is described by Darcy's law.

Henry Darcy was a French hydraulic engineer interested in purifying water supplies using sand filters. He conducted experiments to determine the flow rate of water through the filters. Published in 1856, his conclusions have served as the basis for all modern analysis of ground water flow [27]. The motion of cold water in porous medium is described by Darcy's law:

$$Q = -K\frac{\rho}{\nu}(\Delta P - \rho g)$$

where

$$K = \begin{bmatrix} K_x & 0 & 0 \\ 0 & K_y & 0 \\ 0 & 0 & K_z \end{bmatrix}$$

is the permeability tensor in three dimensions, $Q(kg/sm^2)$ is the fluid flow rate, $\Delta P(Pa/m)$ the pressure gradient, g is the acceleration of gravity and ν the fluid kinematic viscosity. Darcy's law stipulates that the motion of water in porous medium is due to the difference in pressure between two points and/or gravity forces. Capillarity pressure is pressure associated

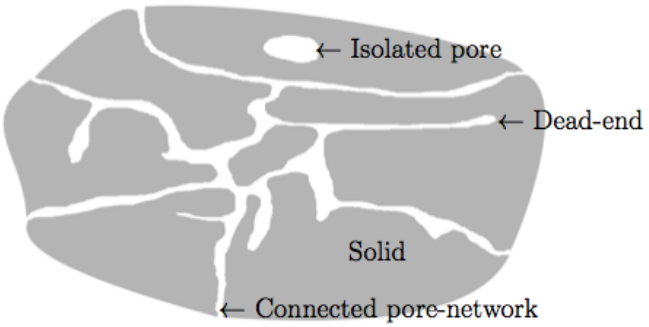

Figure 2.1: A porous medium with a connected network of pores, from [20]

with low porosity, and can be neglected if we assume that fluid is flowing through the porous medium. Darcy's law holds for laminar flow characterised by

$$R_e = \frac{V_{ca} d_{ca}}{\nu}, \quad 1 \leq R_e \leq 10$$

where d_{ca} is the characteristic flow path diameter, V_{ca} the characteristic velocity of the fluid and R_e the Reynolds number. Recall that Reynolds number is the dimensional number measuring the importance of inertial forces versus viscous effects. For low Reynolds number the viscous forces are predominant and the flow is laminar. Darcy's law hold in porous medium but also in fracture medium, since large scale fracture medium can be approximated by porous medium.The pore velocity v_{ca}:

$$v_p = \frac{Q}{\phi}$$

or the interstitial velocity is related to Darcy law by dividing the flow rate Q by the porosity ϕ. The pore velocity v_p would be for example the velocity a conservative tracer would experience if carried by the fluid through the formation

2.1.2 Thermal properties

About 80% of the earth energy is generated by the decay of unstable radio active elements in the crust and the mantle, [26]. The major heat producing elements are Uranium-238, Uranium-235, Potassium-40, and thorium-232. Table 2.1 shows heat production for the major radioactive elements in the crust and mantle. The crust generates hundred times more energy than the mantle per unit volume [26]. However, the rate of energy generation for the entire earth is influenced by the mantle, due to it large volume relatively to the crust, where the fifth of radioactive heat is generated [26]. The total energy of the crust is about $1.4 - 2.7 \times 10^{13} W$ [26]. Due to low matrix and fracture porosity, about 80 to 90% of this energy is stored in the rocks, [18]. The energy generated is mostly transferred through convection and conduction. Radiation is ignored in modelling heat and mass extraction in hydrothermal systems. However, radiation plays an important role in shock wave propagation in hydrothermal systems. Hot fluid moves in the system through convective cells, where fractures are predominant. Consider a volume V_c, V_h of cold and hot water respectively, and associated mass m_c, m_h and density ρ_c, ρ_h. Assuming that the fluid is heated from below,

Table 2.1: Heat producing radioactive elements in the crust and mantle, [26]

Elements	Heat generation (W/kg^{-1})	Quatity (ppb)	Summary
Uranium	9.8×10^{-5}	15-25	Uranium-238 produces 99.28% of the total Uranium energy. Uranium-235 produce 0.72% of the total energy produced by Uranium.
Thorium	2.6×10^{-5}	80-100	Thorium-232 one out of 10^4
Potassium	3.35×10^{19}	150-260	Potassium generates more energy per kg.

the density of the fluid is given by

$$\rho = \rho_0[1 - \alpha(T - T_0) + \beta(P - P_0)].$$

Here ρ_0, T_0, P_0 are some reference density, temperature and pressure, α, T, P are the fluid expansivity, temperature and pressure, respectively, while the compressibility

$$\beta = -\frac{1}{\rho}\frac{d\rho}{dp} = -\frac{1}{V}\frac{dV}{dp}.$$

Sine the fluid density decreases with increasing temperature, we have:

$$m_h = \rho_h V_h \leq \rho_c V_c = m_c.$$

The column of hot water will rise when it is heated from below. As it rises away from the heat source, its temperature decreases and the density of the fluid increases, allowing the column of cold water to fall. This creates a convective cell as depicted in Figure 2.2. Many such cells are responsible for heat transfer in fractured porous medium creating geothermal systems. When rock within the upper mantle and the crust are partially melted, the resulting molten lava, with lower density rises toward shallower depth in the form of magma chamber, dykes, or volcanics discharge, [43]. Conduction is predominant in poorly permeable parts of the crust. In those systems, the microscopic particles undergoes constant oscillations and collisions. The energy generated by this chaotic movement creates a temperature gradient causing heat to flow smoothly from regions of higher temperature to regions of low temperature. This is expressed by Fourier's law

$$\mathbf{q}_f = -\lambda \nabla T \tag{2.1}$$

where $\mathbf{q}_f, \lambda, \nabla T$ are the heat flux density, rock thermal conductivity and temperature gradient, respectively. Unlike conduction, which generates a smooth temperature field, radiation generates jump in the temperature field due to shock wave propagation.

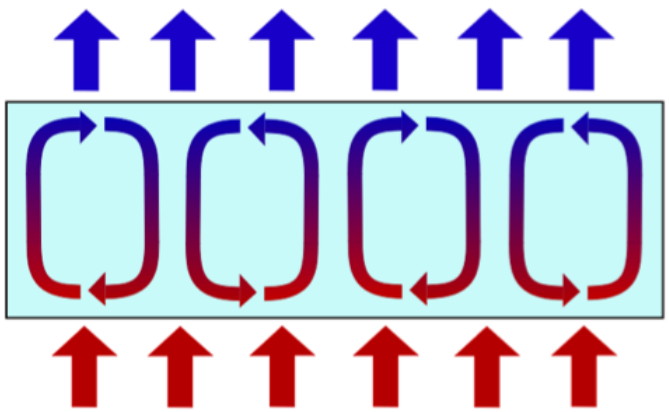

Figure 2.2: A convective cell heated from below, from [20]

2.2 Geothermal Systems

Geothermal energy can be defined as the outward energy flux of the earth, stored in the crust. Most geothermal systems are located along plate tectonics and are associated with volcanic regions as shown in Figure 2.3. Due to a natural geothermal gradient within the crust, geothermal energy can in addition be found anywhere on earth.

A geothermal field is a geographical area with geothermal activity at the earth surface [4]. All hydrological systems directly related to geothermal resources such as fractures zones, heat source, aquifers etc... constitute the geothermal system [4]. The geothermal reservoir is the permeable and hot part of the system [4]. Geothermal systems are classified on the basis of temperature (enthalpy), physical state and their geological setting [4].

Classification based on temperature

On the basis of temperature, geothermal systems can be classified as high temperature systems and low temperature systems. The temperature is at least $200\,^{\circ}\mathrm{C}$ in high temperature systems, while low temperature systems are characterised by temperature below $150\,^{\circ}\mathrm{C}$ [4]. The heat source in high temperature systems is often a hot intrusive magma, formed by incomplete melting of the upper mantle and the crust [4]. High temperature systems are generally situated in volcanic regions. The heat source in low temperature systems, is the hot crust heated by heat conduction and radioactive elements [4, 26].

Classification based on geological formation

On the basis of their geological setting, conventional geothermal systems can be classified as volcanic systems, convective systems, sedimentary systems, Engineered Geothermal Systems (EGS) and shallow geothermal systems [4].

Volcanic systems are located within or in the proximity of volcanic complexes. They are high temperature systems and often involve two phase flow (liquid and steam). The flow of water in volcanic systems is mainly controlled by permeable fractures and fault zones [4]. The heat sources are hot intrusions or magma [4]. *Convective systems* are often situated outside volcanics complex and are predominantly low temperature systems. Characterised by highly fractured rocks, heat is transferred within a convective system through convection

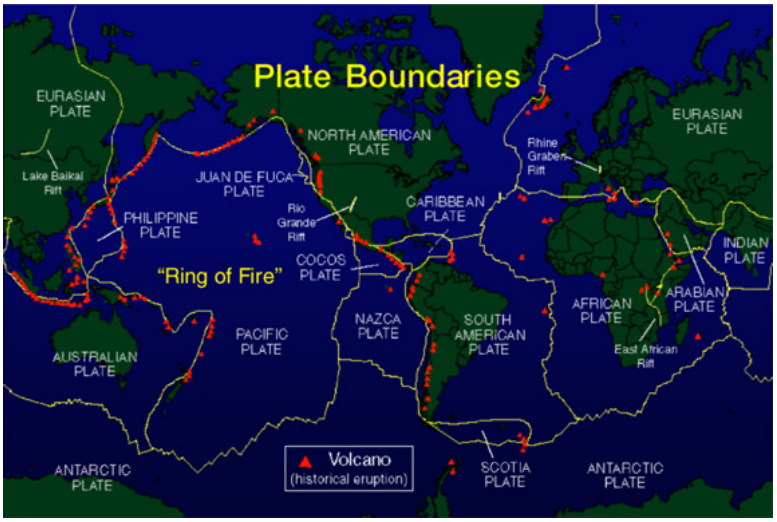

Figure 2.3: Geothermal systems and plate boundaries

cells. *Sedimentary systems* are located in sedimentary basins characterised by permeable sedimentary layers at depth. Heat is transfer mainly through conduction in these systems [4]. An *Engineered Geothermal System* generates geothermal energy without the need for natural convective hydrothermal resources. Through hydraulic stimulation, high pressure cold water is injected into the system, to enhance permeability in the naturally fracture rock. *Shallow geothermal systems* refers to the thermal energy stored near the surface of the earth crust. This energy can be utilised through heat pumps.

Recently abandoned oil and gas wells or dry wells have been investigated for possible sources of geothermal energy. Abandoned oil and gas wells are wells that ceased or never produced oil and gas. They can be as deep as 6000 m [23]. In most geothermal projects the cost of drilling can be as high as 50 $\%$ of the total project cost [21]. By using abandoned oil and gas wells, the cost of geothermal energy production is reduced significantly. To produce geothermal energy from abandoned oil and gas wells, a double pipe heat exchanger can be inserted into a well, as shown in Figure 2.4. A working fluid is injected into one orifice of

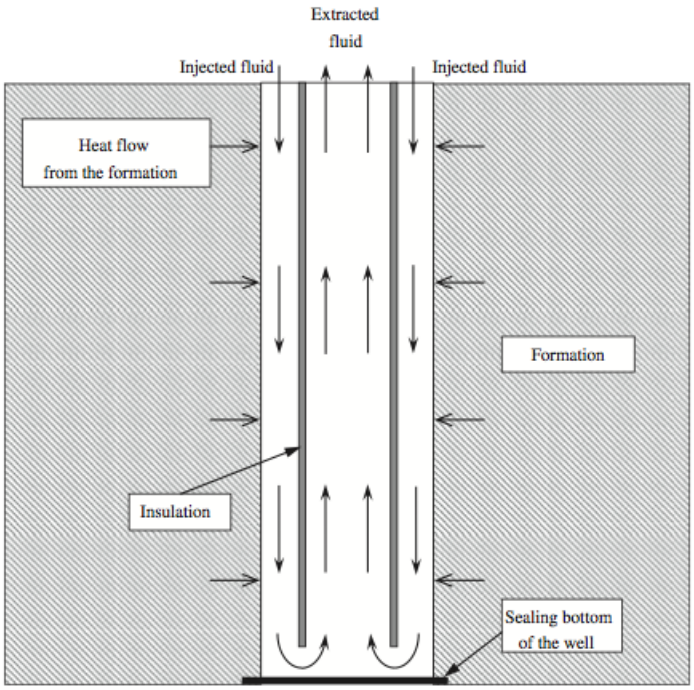

Figure 2.4: Diagram of a double pipe heat exchanger

the heat exchanger. Due to the natural geothermal gradient, the fluid is heated by the geological formation. The recovered geothermal energy depends on the flow rate of the injected working fluid and the geothermal gradient [21, 23]. Computational simulation indicates that the fluid temperature can be around 130 °C or more depending on the working fluid and the geothermal gradient [21]. Organic fluid such as isobutane can be used as working fluid. Due to their low boiling point they are easily converted into high temperature steam [23].

2.3 Geothermal resource assessment methods

Geothermal reservoir engineering is a multidisciplinary field of study. It includes numerical simulation based on geophysics, geology and chemistry. The purpose of geothermal

reservoir engineering is to estimate reservoir properties and production potential, simulate production response and estimate the size of geothermal resources [3]. It plays a key role in resource management.

Geological and geophysical exploration provides some of the basic data for a conceptual model of a geothermal system. The conceptual model is a descriptive model of the system. It incorporates the essentials physical features of the system such as heat sources, hot springs, permeable zones, boundary condition, recharge zones etc [40]. The conceptual model provides an estimate of the reservoir size and describes flow pattern within the system [40]. It is the foundation for a successful numerical simulation. Based on a conceptual model static modelling methods such as volcanic resource assessment can be used to estimate the underground energy in a geothermal system and the likely part of that (10-20 $\%$) that can be extracted over $30 +$ years.

Assessment methods in geothermal reservoir engineering are divided into two: Volumetric assessment methods and dynamics assessment methods [32]. Volumetric assessment methods are used in the the first stage of a geothermal project. Dynamical methods includes simple analytical methods, details numerical simulations and lumped parameters modelling [32]. A combination of volumetric methods and numerical simulation should enhance the reliability of mathematical model of geothermal systems [8]

2.3.1 Exploration methods

Geological methods

The most widely used method is geological mapping. Its goal is to study the viability of a geothermal project. It includes geothermal surface manifestation mapping, surface petrology, mineralogy, lithology, tectonics. It also plays an import role in advanced stages of the project in well siting and well design. A map of surface thermal manifestation such as hot spring, mud pots and warm group can reveal if the geothermal field is active or extinct and delineate its extent [55] .

Geophysical methods

Geophysical methods are import part of geothermal resource assessment. Physical parameters such as density, resistivity and magnetism of the rock are measured. Gravity survey is used to measure density variation, which can for example reveal dense intrusions. Magnetic measurement can give information about dikes [55]. Seismic surveys and seismic monitoring reveals active fracture zones at depth [55]. Gravimetric measurements may reveal tectonic features in the reservoir [55]. Micro gravity monitoring can provide information on the net mass balance of the reservoir (difference between mass withdrawal and the recharge of water) [8]. This includes mass balance from enlarging steam zones and mass balance effect of reinjection. Resistivity surveys reveals temperature distribution of the system and is used to detect regions of permeability and hight temperature zones. It might also help delineate cold fresh water inflow into the geothermal system [8]. The commonly used resistivity survey are Transient ElectroMagnetic (TEM) and MagnetoTelluric (MT) sounding [55].
In TEM survey current is generated in a big loop laying on the ground, see Figure 2.5. By induction the current produces a magnetic field in the ground. By turning off the current abruptly, the varying magnetic field in the ground induces a current. This current is used to map the resistivity structure of the uppermost $1\ km$ of the geothermal system [55].
The MT survey makes use of the natural fluctuations of the earth's magnetic field as depicted

in Figure 2.6. By the principle of induction, the induced current in the earth is measured on the surface by two magnetic dipoles. Because the TM survey uses the natural magnetic field of the earth, it maps the resistivity structure of the geothermal system at greater depth, down tens of km [55].

Chemical methods

Chemical composition of geothermal fluid (steam and water) can reveal the temperature of the reservoir. Changes in fluid chemistry may reveal changes in cold inflow mixing, boiling, etc. It plays an important role in anticipating corrosion and scaling in pipes and wells by identifying corrosive and scaling species. Chemical composition of the fluid can reveal information about the recharge zone of a geothermal reservoir [55]. Change in silica content of water production can for example be interpreted as due to inflow of cold water into the geothermal system [8].

2.3.2 Volumetric assessment method

The volumetric method is used for first stage assessment, when data is scarse. This method is adapted from mineral exploration and oil/gas industry. It is based on estimating the total heat stored in a volume of rock. The thermal energy stored in rock matrix and in water/steam in pore spaces are evaluated. Volumetric method can be applied to individual geothermal system/reservoir, or on a regional scale. For individual systems Monte Carlos method is often applied. The latter involves assigning probability to different parameters by means of

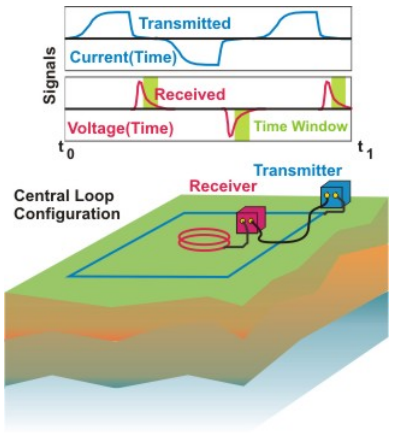

Figure 2.5: TEM survey apparaturs with a central loop, a receiver and a transmitter

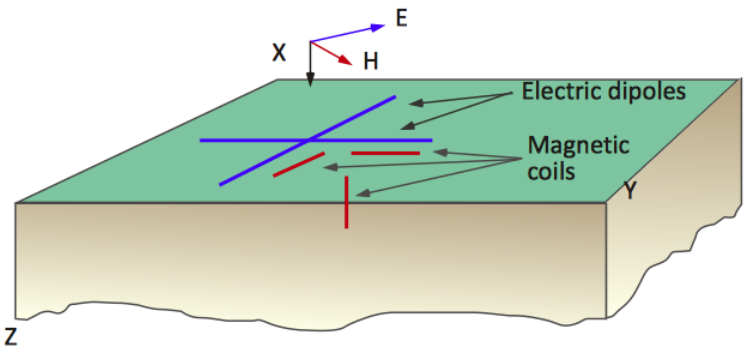

Figure 2.6: MT survey apparatus with magnetic coils and Electric dipoles.

a probability distribution, in order to estimate the system potential with probability.

On a regional scale, all the heat in the Earth's crust below a specific area, commonly down to 10 Km is assessed. This is the geothermal resources base. Below 3 Km, the energy is (at present) inaccessible and above 3 Km the energy, called accessible resources base can be tapped by drilling. The geothermal resource is then the fraction of the resource base that can be extracted economically and legally, at present and up to some future time. The geothermal reserve is then the part of the geothermal resource that can be extracted today at a cost that is competive with other energy sources.

The basic equations for total energy E_{res} for a reservoir, in volumetric assessment method are:

$$E_{res} = E_{rock} + E_{fluid} \tag{2.2}$$

where the energy E_{rock} of rock and E_{fluid} of fluid are respectively

$$E_{rock} = V(1-\phi)\rho_{rock}c_{rock}(T_{res} - T_{ref}), \tag{2.3}$$

$$E_{fluid} = V\phi\rho_{fluid}c_{fluid}(T_{res} - T_{ref}). \tag{2.4}$$

Here ρ_{rock} and ρ_{fluid} are the density of rock and fluid respectively, while c_{rock} and c_{fluid} are the heat capacity of rock and fluid respectively.

For high temperature geothermal systems, volumetric assessment method can be used to estimate the electrical energy generation E_e and power P_e. On the basis of reservoir temperature, the electrical power over some utilisation time Δt, is given by

$$P_e = \frac{E_e}{\Delta t}. \tag{2.5}$$

Here the electrical energy E_e, based on assuming a certain efficiency $\eta \approx 0.008 - 0.1$ is

$$E_e = \eta E_{recovrable} \tag{2.6}$$

where the recovrable energy $E_{recovrable}$ is computed based on the area A of the reservoir, a recovrable factor R, and the reservoir energy given by equation (2.2):

$$E_{recovrable} = ARE_{recovrable}. \tag{2.7}$$

The recovrable factor R indicates how much of the accessible energy may be technically recovered. It is often assumed in the range of $0.05 - 0.20$. In addition to the recovrable energy, the thermal power $P_{thermal}$ can be computed as

$$P_{thermal} = \frac{E_{recovrable}}{\Delta t}. \tag{2.8}$$

On the basis of the reservoir fluid enthalpy h_t, the steam enthalpy h_s and water enthalpy in the reservoir, the electrical power is given by

$$P_e \approx 0.5Q\frac{h_t - h_w}{h_s - h_w} \tag{2.9}$$

where Q is the expected mass flow rate.

The main drawback of the volumetric method is that the dynamic response of a reservoir to production, such as pressure response, is not considered. Reservoirs with same heat content may have different permeabilities and recharge ,and hence, very different production potentials

2.3.3 Dynamic assessment methods

Numerical simulation
Traditionally, conceptual models of geothermal systems are developed on the basis of information from various disciplines including geology, geophysics and geochemistry. Mathematical models are then applied to simulate the behaviour of the system using the conceptual models and data on their response to utilization. [33].

On the basis of the conceptual model constructed from assessment methods described above, a comprehensive mathematical model of the reservoir is constructed. Variables such as pressure, enthalpy, saturation, permeability, storage capacity are often simulated. A successful mathematical model is based on deep understanding of the physical and chemical processes of the system, the boundary condition, the fluid and rock properties, the location of sources and sinks [40]. Fluid flow in geothermal systems can be approximated by flow in a porous medium. The flow is characterised both as single phase (water) or multi-component (carbon-dioxide and NaCl) or multi phase flow consisting of two phases, water and steam [33].

Geothermal systems are modelled in terms of conservation of mass, momentum and energy. A complete model of the system should incorporate the flow of fluid in the reservoir and the production/reinjection wells [33]. The general conservation equations for simulating two phase flow in a geothermal reservoir are given by Grant [24]:
Conservation of mass

$$\phi\frac{\partial}{\partial t}\left(\rho_l S_l f_l + \rho_g S_g f_g\right) + \nabla\cdot\left(\rho_l u_l f_l + \rho_g u_g f_g\right) + q_m = 0, \tag{2.10}$$

where ρ_l, ρ_g, S_l, S_g are the liquid and gas density saturation, respectively and f_l, f_g are the mass concentration of the chemical species in the liquid and gas, respectively. l and g stand for liquid and gas (vapour). u_l and u_g are the liquid and gas velocity given by equations (2.12) and (2.13). q_m is the sink/source term (kg)

Conservation of energy
The conservation of energy is given by

$$\phi\frac{\partial}{\partial t}\left((1-\phi)\rho_r U_r + \phi(\rho_l S_l U_l + \rho_g S_g U_g)\right) + \nabla\cdot(\rho_l u_l h_l + \rho_g u_g h_g - \lambda\nabla T) + q_E = 0 \tag{2.11}$$

where U is the internal energy, h the enthalpy , T the temperature, K the heat conduction coefficient and q_E the sink/source term $(J/m^3 s)$.

Conservation of momentum
The conservation of momentum is given by Darcys law. It describes a linear relationship between the fluids velocity (u_l, u_g) and the pressure gradient relative to the rock:

$$u_l = -\frac{k k_{rl}}{\mu_l}\nabla(P_l - \rho_l g z) \tag{2.12}$$

$$u_g = -\frac{k k_{rg}}{\mu_g}\nabla(P_g - \rho_g g z) \tag{2.13}$$

where k is the absolute permeability, μ_l and μ_g are the dynamic viscosity of liquid and gas respectively, P_l and P_g are the liquid and gas pressure respectively, g is the gravity constant,

z is the vertical depth, k_{rl} and k_{rg} are the relative permeabilities of the rock to the liquid and vapour phase respectively. The above equations hold assuming that capillary pressure effects are neglected.

The steady state equation governing fluid flow in a vertical geothermal well is given by the mass, momentum and energy equation, respectively [15]

$$\frac{\partial m_f}{\partial z} = 0 \tag{2.14}$$

$$\frac{\partial P}{\partial z} - \left(\left(\frac{\partial P}{\partial z} \right)_f + \left(\frac{\partial P}{\partial z} \right)_a + \left(\frac{\partial P}{\partial z} \right)_p \right) = 0 \tag{2.15}$$

$$\frac{\partial E}{\partial z} \pm q_f = 0 \tag{2.16}$$

with

$$E = m(Xh_g + (1-X)h_l + 0.5(Xu_g^2 + (1-X)u_l^2) + g(L_w - z)) \tag{2.17}$$

where q_f is the heat flux, m_f is the mass flow rate, X is the mass fraction of steam or dryness, h_l and h_g are the liquid and gas (steam) enthalpies respectively, z is the vertical coordinate axis, L_w is the depth of the well and $\left(\frac{\partial P}{\partial z}\right)_f, \left(\frac{\partial P}{\partial z}\right)_a, \left(\frac{\partial P}{\partial z}\right)_p$ are the pressure gradients due to frictional, acceleration and potential forces along the well respectively. They are given respectively by

$$\left(\frac{\partial P}{\partial z} \right)_f = \varphi^2 \left(\frac{f_{lo} G^2}{4 r_w \rho_l} \right) \tag{2.18}$$

$$\left(\frac{\partial P}{\partial z} \right)_a = G(Xu_g + u_l(1-X)) \tag{2.19}$$

$$\left(\frac{\partial P}{\partial z} \right)_p = \rho m g \tag{2.20}$$

where G is the mass velocity, r_w is the well radius, u_l and u_g are the liquid and gas (steam) velocities respectively, f_{lo} is the liquid friction factor, φ^2 is the two phase multiplier given by

$$\varphi^2 = 1 + \left(\Gamma^2 - 1\right)\left(B_r X(1-x) + X^2\right)$$

with

$$\Gamma^2 = \frac{\rho_l}{\rho_g} \tag{2.21}$$

$$B_r = B_s \left(\frac{1}{2} \left(1 + \left(\frac{\mu_g}{\mu_l} \right)^2 10^{-\frac{300\epsilon}{r_w}} \right) \right)$$

where B_s is obtained from Table 2.2 and ϵ is the pipe roughness. For constant mass flow rate m, equations (2.14), (2.15) and (2.16) can be solved for pressure P and steam quality x by using Newton method for system of nonlinear equations [15].

Equations governing the behaviour of a geothermal system can be solve numerically by various softwares. Software for geothermal system simulation fall into two categories:

Reservoir and wellbore simulation software. The most widely used reservoir simulator are THOUGH2 and its family, STAR and TETRAD [42, 44, 51, 32]. The THOUGH2 family are designed to simulate the coupled transport of fluid, heat and chemical species for multi phase flow in porous and fracture media [44]. The conservation equations are discretised in space using the integral finite difference method [25, 53, 33]. The time derivative is discretised using a finite difference scheme (backward, forward, centered). Due to the fact that THOUGH2 is discretised using an integral finite difference method, it has the advantage of handling unstructured meshes (see Figure 2.7) as opposed to STAR and TETRAD. This makes THOUGH2 the facto reservoir simulation software [32]

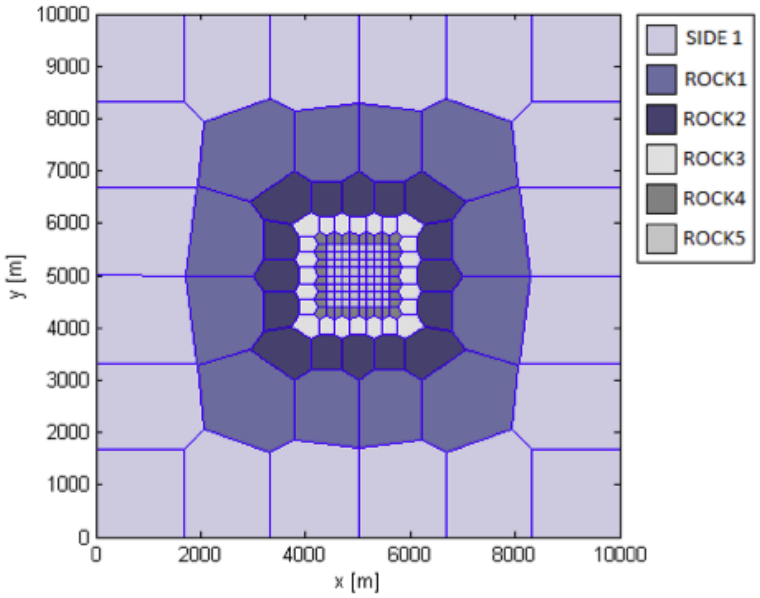

Figure 2.7: Unstructured mesh generated by THOUGH2. Taken from [32]

Table 2.2: Different values of B_s based on Γ (2.21) and G

Γ	$G(\frac{kg}{m^2 s})$	B_s
≤ 9.5	≤ 500	4.8
	$500 \leq G \leq 1900$	$\frac{2400}{G}$
	≥ 1900	$\frac{55}{G^{0.5}}$
$9.5 < \Gamma < 28$	≤ 600	$\frac{520}{\Gamma G^{0.5}}$
	> 600	$\frac{21}{\Gamma}$
≥ 28		$\frac{15000}{\Gamma^2 G^{0.5}}$

The first wellbore softwares were designed to solve steady state conservation equations [29, 32]. The first simulator capable of handling unsteady state conservation equation was WELBORE designed by Miller [32, 38]. All these softwares solved the conservation equations from bottom to top along the well or vice versa, without incorporating the feed zones in the wells. The first software able to handle one feed zone was the software BROWN [14, 32]. HOLA was the first simulator capable of handling multiple feed zones in the well [15].

Successful simulation of a geothermal system is based on coupling empirical data and numerical simulation. The verification process maps the measured data from the system to the results obtained from mathematical modelling. Verification is done through calibration [40]. If the error between the measured and the calculated solution falls within an acceptable range, the simulation is a success. In this case the mathematical model represents a fairly good approximation of the system. O'Sullivan developed a general method of model calibration [40]. It consists of natural state modelling followed by history matching. In natural state modelling, the model is run for a long period of time to mimic the natural behaviour of the system and its steady state before production starts [40]. The simulated variables are compared with the measured field data. Some parameters of interest such as permeability structure, location of the heat source of the model are adjusted to obtain the minimum possible discrepancy between measured and simulated data [40]. This step does not take into account the production history of the system. For system with production history, the measured behaviour of the geothermal field is matched with the simulated behaviour in response to production [40].

Lumped parameters modelling and analytical method

A lumped parameter modelling software was designed by Axellsson to simulate the pressure changes in a low temperature geothermal well [5]. The methods consist of approximating the permeability and the storage capacity of the reservoir by lumped parameters. By using inverse modelling the analytical response of the reservoir is mapped with measured data. Simple analytical methods can also be used to model fluid flow in geothermal reservoir. Lumped parameter modelling is described in more detail in a later chapter.

2.4 Reinjection in geothermal systems

2.4.1 Historical background and advantages

Reinjection in geothermal resource management consists of injecting the used geothermal water back into the reservoir. Water of different origins such as surface water and sewage water can also be injected [2]. It started as a way of disposing of the waste water from geothermal energy utilisation [2]. The first recorded instance of injection of energy depleted water into a high temperature reservoir is in the Ahuachapan field in El Salvador in 1969 [2, 50]. At the same time the use of long term reinjection was implemented successfully in the Dogger limestone reservoir located in the Paris basin [2]. The Dogger reservoir stretching 150000 km^2 is mainly used for district heating. The production and reinjection wells are separated by a distance of about $1km$. The reinjection scheme in the Paris basin lasting 30 to 40 years has indicated no significant cooling of production wells due to cold water injection [2]. In 1970, operators in the Geyser geothermal field started to inject the steam condensate, and realised that this process increased the reservoir performance [2]. Since then reinjection has been an integrant part of resource management in the Geyser field. It

was later observed that due to the injection process, the decline of electrical production at the Geyser was considerably slower than before [2, 49].
In Italy reinjection started in 1974 in the Larderello field as a means to dispose of the steam condensate [2, 22, 50]. The long term production history has revealed that since reinjection started, steam production along with pressure have increased in the Lardelerollo geothermal field [2, 50], See Figure 2.8.

Reinjection started in Iceland in 1997 at the Laugaland low temperature field in north Iceland [8]. In the Laugaland geothermal system 10 to 20% of the extracted mass are reinjected [8, 2]. In the Hofstadir geothermal system in West Iceland reinjection started in 2006. About 40 to 50% of the extracted mass are reinjected back into the system [2]. Due to the low chemical content in most Icelandic geothermal field and the good recharge of water, reinjection started relatively late in Iceland [2]. Now reinjection is practiced in most of the hight temperature fields in Iceland. It is estimated that the number of geothermal field in which reinjection is a part of resource management is likely more than 60 [2].

Reinjection is a vital part of an Enhanced Geothermal System (EGS) [2]. An EGS is a man made reservoir, created where there is hot rock but insufficient or little natural permeability or fluid saturation. About 80 to 90% of the energy of a geothermal reservoir is stored in the rock [2, 26]. Therefore in an EGS, fluid is injected into the system at a sufficient pressure to create a fracture network into the rock with sufficient permeability, see Figure 2.9. A production well is drilled into the fracture network to intersect the created flow paths. The production capacity of a geothermal system is mainly controlled by pressure response [4]. During reinjection, the reservoir pressure is increased significantly, therefore reinjection increases the production capacity of the reservoir. As an environmental protection tool, it is a way of disposing the high chemical content of geothermal waste water. It mitigates surface subsidence and can be used to maintain the integrity of surface activities [2].
Reinjection can however affect the lifetime efficiency of the reservoir. The lifetime efficiency η of a reservoir given by

$$\eta = \frac{E_r}{E_T},$$

can be defined as the ratio of the heat produced over it life time to the total available heat content of the reservoir [46]. Here E_r and E_T are the heat produced by the reservoir over it life time and the total available heat content, respectively. The injected water is generally

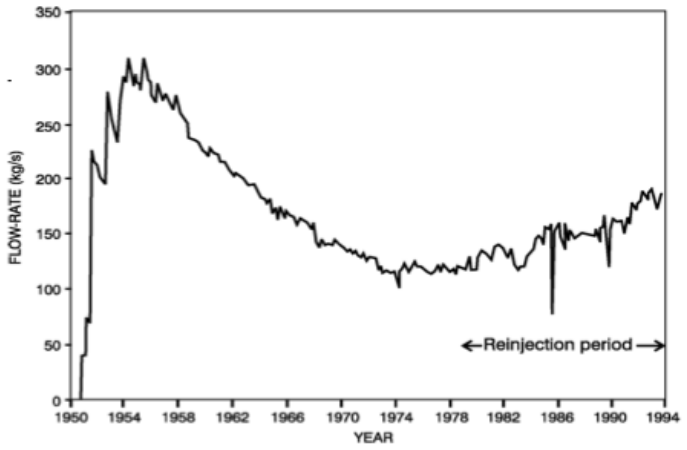

Figure 2.8: Flow rate history at the Larderello field [22]. Taken from [2]

colder than the reservoir rock and can intersect fractures to create a premature cold water inflow, cooling down the reservoir and decrease the reservoir efficiency. Reinjection can create and reopen pre-existing fractures. If created or reopen fractures intersect a cold aquifer, cold water breakthrough can be induced into the reservoir. Due to a large amount of fluid being injected into the reservoir, pressure increase can cause rock to slip along pre-existing fractures and produce microseismic events. In addition, silica scaling in high temperature systems, carbonate scaling in low temperature systems, corrosion in pipelines and injection wells can be problems associated with injection. Clogging of aquifers next to injection wells in sandstone reservoir can also be a significant problem [2]. To mitigate the problems associated with reinjection, a careful reinjection scheme must be designed.

2.4.2 Mitigating problems associated with reinjection

To avoid premature thermal breakthrough and increase the efficiency of the reservoir through injection, the injection scheme must ensure the optimum distance between injection wells and production wells [2, 46]. Thermal breakthrough has been observed in relatively few geothermal systems worldwide [2, 50]. In the Palinpinon geothermal system in the Philippines, thermal breakthrough occurred about 18 months after reinjection started, as an example. The temperature dropped by about $50\,^{\circ}\mathrm{C}$ over a period of 4 years [2]. To circumvent this problem, tracer testing can for example be used to locate fracture zones, flow path and determine the thermal front velocity to predict any premature thermal breakthrough. Analytical method can also be used to estimate thermal front velocity, as presented later in this work.

2.4.2.1 Tracer testing

Tracer testing is the most powerful tool for studying connections between injection and production wells and to predict thermal breakthrough [9]. It involves injecting a chemical tracer into the geothermal system, and monitoring its recovery through time at various points. The

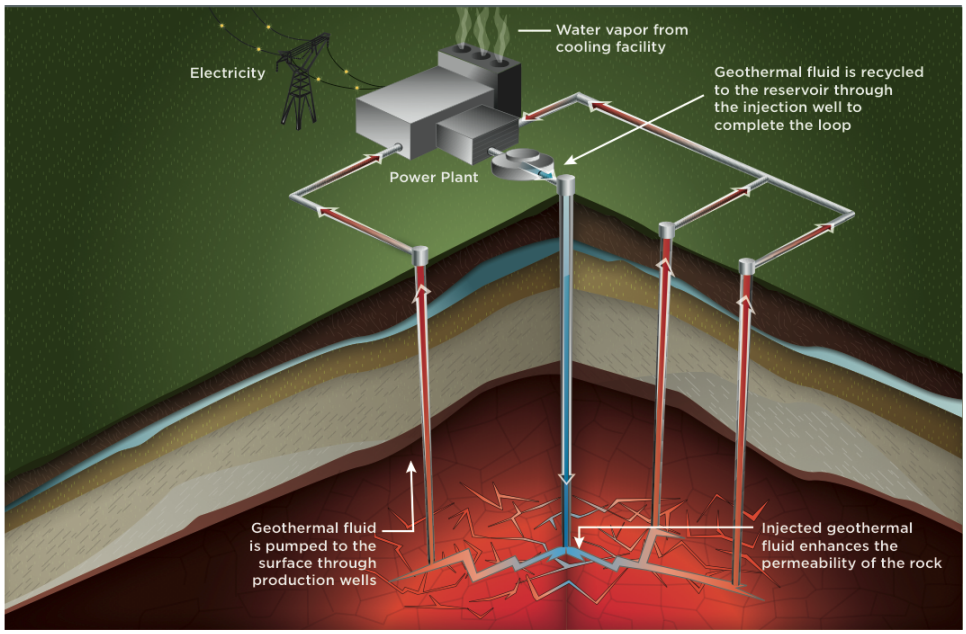

Figure 2.9: Schematic description of an EGS

chemical tracer arrival time and the thermal breakthrough time are proportional by $2-3$ order of magnitude [2]. Therefore determining the tracer arrival time gives approximately the thermal breakthrough time. Three types of tracer are commonly used in geothermal application: Radioactive tracers such as Iodine-125, Iodide-131 and Tritium, Fluorescent tracer such as rhodamine WT and chemical tracer such as iodide and bromide [7].

Assuming that a tracer of mass M is injected at $t = 0$ with injection rate q into a one dimensional channel (see Figure 2.10) with cross sectional area A, connecting an injection well and a production well, with porosity ϕ, dispersion coefficient D and fluid density ρ, the concentration C of the tracer is modelled by [7]:

$$\frac{\partial C}{\partial t} + \frac{q}{\rho A \phi}\frac{\partial C}{\partial x} - D\frac{\partial^2 C}{\partial x^2} = 0. \tag{2.22}$$

The theoretical response given by [7]

$$C(t) = \frac{4M\rho}{Q}\frac{1}{2\sqrt{\pi D t}}\exp\left(-\frac{x-4t}{4Dt}\right) \tag{2.23}$$

is simulated with the tracer data to obtain the flow channel volumes $Ax\phi$ and the longitudinal dispersivity α_L [7]. In equation (2.22) and (2.23), $D = \alpha_L \frac{q}{\rho A \phi}$, Q is the production rate of the production well.

The software TRINV included in the ICEBOX software package developed at Iceland GeoSurvey uses non linear least squares fitting to simulate data and return the flow channel volumes and the dispersivity [7]. Once equation (2.23) is fully defined, the concentration profile $C(t)$ can be use to determine the arrival time of the tracer concentration C.

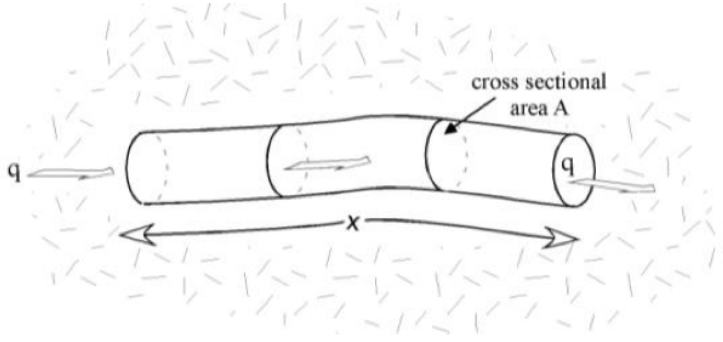

Figure 2.10: One dimensional flow channel connecting injection well and production well [7]

Chapter 3

Model of thermal front velocity induced by cold water injection

The underlying physics of a geothermal system is rather complex due to the complex nature of its mechanical and thermal properties. Hot fluid circulates through porous fractured rock containing thermal energy. The mathematical description of such a complex system is achieved by making assumptions that simplify the behaviour of the system. These mathematical models can be represented by differential equations that can be solved analytically for simple models or numerically for complex models.

The temperature distribution of a low enthalpy geothermal reservoir undergoing cold water injection can for example be formulated in terms of conservation laws. The cold front velocity induced during injection has been computed by Stopa and Wajnarowski in [48]. Their result was obtained from conservation of energy and the method of characteristics, applied to an initial boundary value problem. The resulting computed thermal front velocity is expressed as a weighted average of the derivative of the flux function. In this thesis we present a new analytical method for computing the thermal front velocity by solving the Riemann problem. We show that the unique solution, which represents the temperature front, moves at the speed equal to the thermal front velocity. This result is predicted by the theory of hyperbolic conservation laws [34] and is computed from the Rankine-Hugoniot shock condition. It is expressed as the average value of the derivative of the flux function over the interval defined by the injected water temperature and the reservoir temperature. A relative error of magnitude 10^{-3} was observed between the new approach and the one presented in [48] .

Reinjecting colder fluid into a hot reservoir is an integral part of resource management [2, 4]. Due to the cold temperature of the injected fluid, however, cooling of the production wells can occur, as observed in Beowawe, Nevada and the Geysers geothermal reservoir [41, 37]. To mitigate this cooling effect, predicting the velocity of the cold water movement, is an essential part of the reinjection scheme. Assuming 100% fluid return rate from the injection well to the production well, Bodvarsson [17] was the first to derived the thermal front velocity for constant fluid and rock properties, using the characteristics method. This technique produces a non physical solution when the rock and fluid properties are temperature dependent. By using the characteristics method, Stopa and Wajnarowski extended Bodvarsson work by solving an initial-boundary value problem for the conservation laws [48]. They derived the thermal front velocity by using conservation of energy. In this thesis, we present an alternative approach.

In the new approach we formulate the injection problem as the well-posed Riemann problem described by the well established theory of hyperbolic conservation laws. Rather than using the method of characteristics, we solve an initial problem as opposed to the initial-boundary problem of Stopa and Wajnarowski. By doing so we transform the injection problem to the well known Riemann problem. The unique solution for the Riemann problem [34], propagates at a speed equal to the thermal front velocity. By revisiting the findings of Bodvarsson, Stopa and Wajnarowski in [48], we compare the thermal front velocity obtained by Bodvarsson and by Stopa and Wajnarowski in [48] with the one predicted by the theory of hyperbolic conservation laws, which we call the Riemann method. This Chapter starts by presenting the governing equations for the thermal front velocity model, followed by the early work of Bodvarsson and the recent work by Stopa and Wajnarowski. The new method (the Riemann method) is later presented. The Chapter ends with a comparison between the different methods and the limitations of the current models. The thermal front velocities computed in this Chapter are later applied to a case study in Chapter 5 where a low temperature geothermal system located in west Iceland is model.

3.1 Governing equation

A single phase(liquid) fluid flow in porous medium is govern by the conservation of mass and energy equation similar to the one described in Chapter 2 and given by [54]:

$$\frac{\partial(\phi\rho_w(u))}{\partial t} + \frac{\partial}{\partial x}(\rho_w(u)u_w) = 0 \tag{3.1}$$

$$\phi\frac{\partial}{\partial t}\left(\phi\rho_w(u)c_w(u)u + (1-\phi)\rho_r(u)c_r(u)u\right) + \frac{\partial}{\partial x}(\rho_w(u)c_w(u)u_w u) = \lambda\frac{\partial^2 u}{\partial x^2} \tag{3.2}$$

In the literature describing conservation laws, u is used to defined the conserve quantity. In the same fashion, in this chapter we define u as the temperature. $c_w(u), c_r(u), \rho_w(u), \rho_r(u)$ are the heat capacity of water/rock and density of water/rock respectively, ϕ, u_w, λ are the porosity, the Darcy velocity of liquid phase and the heat conduction coefficient respectively. Darcy velocity u_w is normally pressure dependent. Therefore equations (3.1) and (3.2) represent a system of two equations with two unknowns.

To simplify the system of equations (3.1, 3.2), equation (3.2) is expended and the conservation of mass (3.1) is used in order to get one equation [48]. By expending (3.2) we get

$$\begin{aligned} c_w(u)u\left(\frac{\partial\phi\rho_w(u)}{\partial t} + \frac{\partial}{\partial x}(\rho_w(u)u_w)\right) + \frac{\partial}{\partial t}((1-\phi)\rho_r(u)c_r(u)u) \\ +\phi\rho_w(u)\frac{\partial}{\partial t}(c_w(u)u) + \rho_w(u)u_w\frac{\partial}{\partial x}(c_w(u)u) = \lambda\frac{\partial^2 u}{\partial x^2}0. \end{aligned} \tag{3.3}$$

Using (4.2), the first expression in (3.3) vanishes and we end up with

$$\frac{\partial}{\partial t}((1-\phi)\rho_r(u)c_r(u)u) + \phi\rho_w(u)\frac{\partial}{\partial t}(c_w(u)u) + \rho_w(u)u_w\frac{\partial}{\partial x}(c_w(u)u) = \lambda\frac{\partial^2 u}{\partial x^2}. \tag{3.4}$$

Applying the chain rule on (3.4) and assuming that Darcy velocity u_w is constant, after rearranging the terms we end up with

$$\frac{\partial u}{\partial t} + \frac{u_w}{\phi} F(u) \frac{\partial u}{\partial x} = \left(\frac{\lambda}{(1-\phi)\left(\frac{\partial(\rho_r(u)c_r(u)u)}{\partial u}\right) + \phi\rho_w(u)\left(\frac{\partial(c_w(u)u)}{\partial u}\right)} \right) \frac{\partial^2 u}{\partial x^2} \tag{3.5}$$

or

$$\frac{\partial u}{\partial t} + \frac{\partial G(u)}{\partial x} = \left(\frac{\lambda}{(1-\phi)\left(\frac{\partial(\rho_r(u)c_r(u)u)}{\partial u}\right) + \phi\rho_w(u)\left(\frac{\partial(c_w(u)u)}{\partial u}\right)} \right) \frac{\partial^2 u}{\partial x^2} \tag{3.6}$$

where

$$G(u) = \frac{u_w}{\phi} \int_0^u F(x)\mathrm{d}x$$

$$F(u) = \frac{\phi\rho_w(u)\left(\frac{\partial(c_w(u)u)}{\partial u}\right)}{(1-\phi)\left(\frac{\partial(\rho_r(u)c_r(u)u)}{\partial u}\right) + \phi\rho_w(u)\left(\frac{\partial(c_w(u)u)}{\partial u}\right)} \tag{3.7}$$

and from [48] the temperature (u) dependent heat capacity of water $c_w(u)$, heat capacity of rock $c_r(u)$, density of water $\rho_w(u)$ and density of rock $\rho_r(u)$ are respectively

$$c_w(u) = \frac{1}{0.00023749816 + 8.0681767 * 10^{-8}u - 8.0367134 * 10^{-10}u^2}$$

$$c_r(u) = 1234.257 - 454.546\exp(-0.00397334833482u)$$

$$\rho_w(u) = 1043.196 - 42.966623\exp(0.00689550122u)$$

$$\rho_r(u) = \frac{2650}{1 + (u-20)0.5 * 10^{-4}}.$$

If we neglect conduction as second order effect by setting $\lambda = 0$ in (3.6), we obtain

$$\frac{\partial u}{\partial t} + \frac{\partial G(u)}{\partial x} = 0. \tag{3.8}$$

Equation (3.8) is a hyperbolic conservation laws and is the same equation as derived in [48]. From the theory of hyperbolic conservation laws, function $G(u)$ is called the flux function [34]. In this application $G(u)$ is the energy flux. Equation (3.8) describes transport phenomenon; in this case transport of heat. Recall that $u = u(x,t)$ is the temperature and according to (3.8) the temperature is conserved. To see this, we can integrate over a given closed interval $[a,b]$ and get:

$$\frac{\partial}{\partial t}\int_a^b u(x,t)\mathrm{d}x = \int_a^b \frac{\partial}{\partial t}u(x,t)\mathrm{d}x \tag{3.9}$$

$$= -\int_a^b \frac{\partial}{\partial x}G(u(x,t))\mathrm{d}x \tag{3.10}$$

$$= G(u(a,t)) - G(u(b,t)) \tag{3.11}$$

$$= [\text{inflow at a}] - [\text{inflow at b}] \tag{3.12}$$

Therefore the physical quantity modelled by u, is neither created nor destroyed: The total amount of u contained inside any given interval $[a,b]$ can change only due to the flow of u across boundary points a, b. It is well known from the literature that equations of type (3.8)

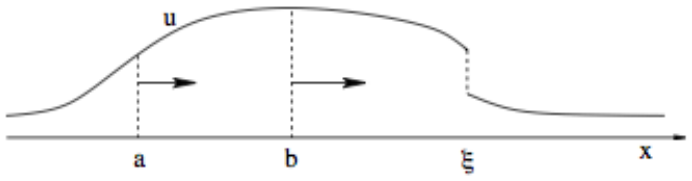

Figure 3.1: Flow across point a and b with discontinuity at ξ

admit discontinuous solutions [34]. Assume now that u has a jump or discontinuity at ξ as shown in Figure 3.1. Then (3.8) is meaningful only in a class of discontinuous or generalised functions. Solutions must therefore be interpreted in distributional sense. We therefore say that u is a solution of (3.8) if

$$\int\int (u\phi_t + G(u)\phi_x)\mathrm{d}x\mathrm{d}t = 0 \tag{3.13}$$

for every infinitely continuous differentiable function ϕ with compact support. Equation (3.13) is the weak formulation of (3.8). We only require that u and $G(u)$ be locally integrable. This is a weaker requirement then continuity. To sum up, the problem of injecting colder water into a hot geothermal reservoir can be modelled by

$$\frac{\partial u}{\partial t} + \frac{\partial G(u)}{\partial x} = 0 \tag{3.14}$$

with initial data

$$u(x,0) = u_0(x) \tag{3.15}$$

This model assumes that the geological formation exhibit mainly micro permeability due to very small intergranular openings [17]. It means that the reservoir is assumed homogeneous isotropic porous and permeable media, saturated with incompressible fluid. The fluid is percolating through the reservoir rock. At any given point, the fluid and the reservoir have the same temperature.

The injection of energy depleted water into a hot geothermal reservoir, was first studied by Bodvarsson for temperature independent fluid and rock properties [17]. He found that the temperature field was transported through the porous media at a rate given by the thermal front velocity. The model and method provided by Bodvarsson was later extended to temperature dependent fluid and rock properties by Stopa and Wajnarowski. In this thesis, we provide an alternative method called the Riemann method, to compute the thermal front velocity for temperature dependent fluid and rock properties. The results obtained from Bodvarsson, Stopa and Wajnarowski and the Riemann method, are applied in Chapter 5, to compute the thermal front velocity induced from cold water injection in the Munadarnes geothermal system, located in west Iceland.

3.2 Early work on thermal front velocity

We consider a geothermal reservoir with temperature u_r and injected water of temperature u_l at $t = 0$. Assume that $u_l < u_r$. We are interested in the temperature distribution of the reservoir and the rate at which the colder injected water propagates through the reservoir.

Ultimately we can calculate the distance travelled by the cold injected water with time. The thermal front velocity is defined as the rate at which the cold injected fluid moves through the reservoir rock. Bodvarsson first formulated this problem for constant rock and fluid properties by solving [17, 48]

$$\frac{\partial u}{\partial t} + \underbrace{\left(\frac{u_w}{\phi}\frac{\phi\rho_w c_w}{(1-\phi)\rho_r c_r + \phi\rho_w c_w}\right)}_{\textbf{W=Constant}}\frac{\partial u}{\partial x} = 0 \tag{3.16}$$

with initial and boundary condition given by a function g,I

$$u(x,0) = g(x), \quad u(0,t) = I \tag{3.17}$$

where c_w, c_w, ρ_w, and ρ_r are the temperature independent heat capacities and densities of water and rock, respectively. Darcy velocity and porosity are respectively, u_w and ϕ. By using the method of characteristics also called characteristics method, Bodvarsson was able to compute the thermal front velocity. The characteristics of equation (3.16) are parametrized curves along which the solutions of (3.16) are constant. The characteristic equations of equation (3.16) for a parameter s are given by

$$\frac{dx}{ds} = W \tag{3.18}$$

$$\frac{dt}{ds} = 1 \tag{3.19}$$

$$\frac{dz}{ds} = 0. \tag{3.20}$$

By solving equations (3.18), (3.19) and (3.20) we get respectively

$$x(s) = Ws + C_1 \tag{3.21}$$

$$t(s) = s + C_2 \tag{3.22}$$

$$z(s) = C_3 \tag{3.23}$$

where W is the constant given in equation (3.16) and C_1, C_2 and C_3 are arbitrary integration constants. By eliminating the parameter s in (3.21), (3.22) and (3.23) respectively, we get the characteristics equation

$$x - Wt = C_0 \Longrightarrow x(t) = Wt + C_0 \tag{3.24}$$

where C_0 is a constant that can vary. Let show that the solution $u(x,t)$ of equation (3.16) is constant along the characteristics. By substituting equation (3.24) into equation (3.16) and applying the chain rule we obtain

$$\begin{aligned}\frac{du(x(t),t)}{dx} &= \frac{\partial u(x(t),t)}{\partial t} + \frac{\partial x(t)}{\partial t}\frac{\partial u(x(t),t)}{\partial x} \\ &= \frac{\partial u}{\partial t} + W\frac{\partial u}{\partial x} \\ &= 0\end{aligned} \tag{3.25}$$

From Figure 3.2 we can observe that the characteristic lines are parallel. The solution of

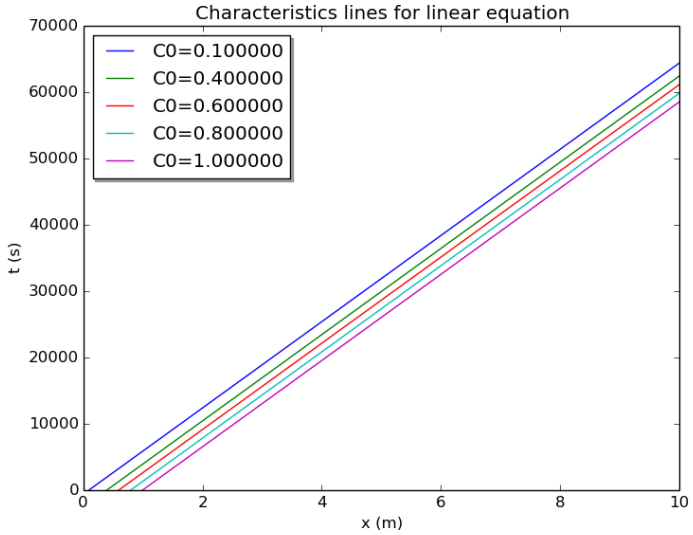

Figure 3.2: Characteristics for different values of C_0 with $W = 1.5 \times 10^{-4}$ SI unit

Table 3.1: Fluid and rock properties used for computing W, with $\phi = 0.15$, $u_w = 10^{-4}$

Temperature (°C)	c_r $(J/Kg.°C)$	c_w $(J/Kg.°C)$	ρ_r (Kg/m^3)	ρ_w (Kg/m^3)	W (m/s)
80	903	4187	2642	968.6	1.5×10^{-4}

equations (3.16), (3.16) is then given in terms of the characteristics as

$$u(x,t) = g(x - Ct) \tag{3.26}$$

where g is the initial condition. For discontinuous initial function g, the solution of (3.16), computed by Bodvarsson, is given by Figure 3.3. The thermal front velocity can now be computed as the speed at which the characteristics given by equation (3.24) move, by taking the time derivative of the characteristics equation:

$$\begin{aligned} \frac{dx(t)}{dt} &= W \\ &= \left(\frac{u_w}{\phi} \frac{\phi \rho_w c_w}{(1-\phi)\rho_r c_r + \phi \rho_w c_w} \right). \end{aligned} \tag{3.27}$$

Figure 3.3 shows the thermal front velocity moving at the constant velocity W. Table 3.1 shows the numerical value of the thermal front velocity W when the reservoir is at $80°C$. The characteristics method works as long as the characteristic lines are parallel. This is due to the fact that the solutions of equation (3.16) are constant along the characteristic lines. If characteristics collide, equation (3.16) will admit multivalued solutions, which are not physical.

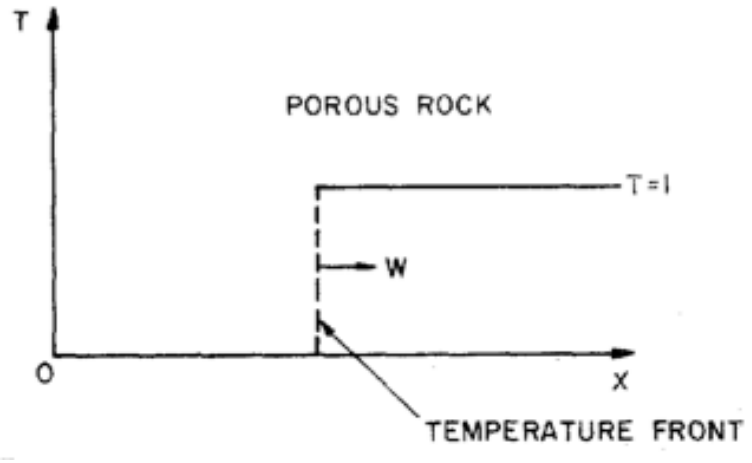

Figure 3.3: Thermal front moving with velocity w from [17]

3.3 Recent work on thermal front velocity

Stopa and Wajnarowski extended the work of Bodvarsson to include temperature dependent fluid and rock properties. In this case equation (3.14) can be rewritten as

$$\frac{\partial u}{\partial t} + \frac{u_w}{\phi} F(u) \frac{\partial u}{\partial x} = 0 \tag{3.28}$$

with initial and boundary condition

$$u(x,0) = u_r, \quad u(0,t) = u_l \tag{3.29}$$

where

$$F(u) = \frac{\phi \rho_w(u) \left(\frac{\partial (c_w(u)u)}{\partial u} \right)}{(1-\phi) \left(\frac{\partial (\rho_r(u) c_r(u) u)}{\partial u} \right) + \phi \rho_w(u) \left(\frac{\partial (c_w(u)u)}{\partial u} \right)}. \tag{3.30}$$

By applying the characteristics method as in the earlier section, we get the characteristics equation for equation (3.28):

$$x = \frac{u_w}{\phi} F(c_0) t + c_0 \tag{3.31}$$

where c_0 is a constant that can vary. Let show that there is a time t^* at which the characteristics will collide. Let c_0 and c_1 be two constants associated to two characteristics

$$x = \frac{u_w}{\phi} F(c_0) t^* + c_0$$

$$x = \frac{u_w}{\phi} F(c_1) t^* + c_1.$$

Since the slops of these characteristic lines are different, by solving

$$\frac{u_w}{\phi} F(c_0) t^* + c_0 = \frac{u_w}{\phi} F(c_1) t^* + c_1$$

we see that the two characteristics will collide at

$$t^* = \frac{\phi (c_0 - c_1)}{(F(c_1) - F(c_0)) u_w}.$$

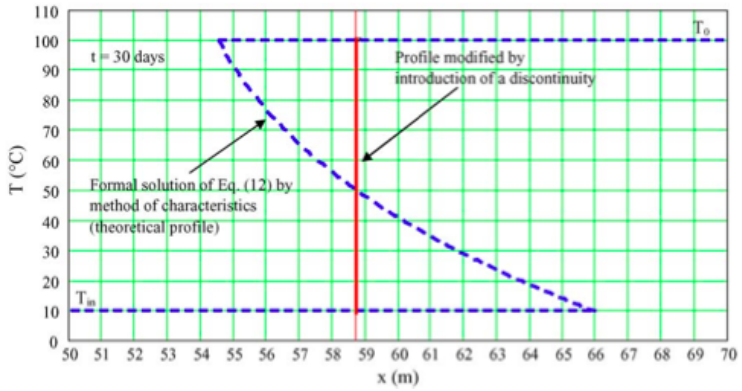

Figure 3.4: Non physical solution obtained in [48] from the method of characteristics

At $t \geq t^*$, the solution $u(x,t)$ is no longer a single valued function and equation (3.28) with boundary and initial condition given by (3.29) has no unique solution. Figure 3.4 shows the solution of equations (3.28), (3.29) produced by the characteristics method. To select the unique solution, Stopa and Wajnarowski proposed conservation of energy. They argue that, since the solution is a discontinuity, the position z of the discontinuity which allows uniqueness must be selected such that energy is conserve in the system. Conservation of energy is then formulated as:

$$t\frac{u_w}{\phi}\int_{u_l}^{u_r} U(u)F(u)\mathrm{d}u = z\int_{u_l}^{u_r} U(u)\mathrm{d}u, \tag{3.32}$$

and setting $v_{TF} = \frac{z}{t}$ as the thermal front velocity, they obtained

$$v_{TF} = \frac{u_w}{\phi}\left(\frac{\int_{u_l}^{u_r} U(u)F(u)\mathrm{d}u}{\int_{u_l}^{u_r} U(u)\mathrm{d}u}\right) \tag{3.33}$$

where the internal energy $U(u)$ is given by [48]

$$U(u) = (1-\phi)\rho_r(u)(u)c_r(u) + \phi\rho_w(u)c_w(u). \tag{3.34}$$

The variation of internal energy $U(u)$ with temperature u is given in Figure 3.5. The thermal front velocity obtained by Stopa and Wajnarowski is the weighted average of the derivative of the flux function :

$$G(u) = \frac{u_w}{\phi}\int_0^u F(x)\mathrm{d}x \implies \frac{dG(u)}{du} = \frac{u_w}{\phi}F(u)$$

So that (3.33) can be written as

$$v_{TF} = \left(\frac{\int_{u_l}^{u_r} U(u)G'(u)\mathrm{d}u}{\int_{u_l}^{u_r} U(u)\mathrm{d}u}\right) \tag{3.35}$$

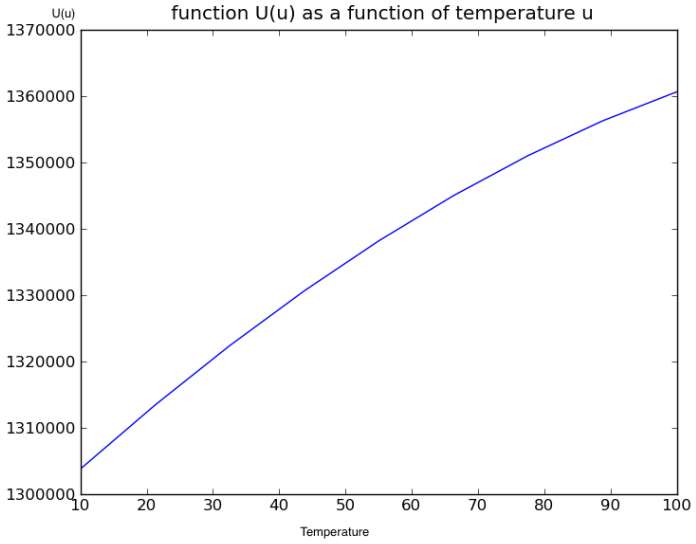

Figure 3.5: Internal energy U as a function of temperature $u(in\,^{\circ}\mathrm{C})$ defined in 3.34

3.4 The new method for computing the thermal front velocity: The Riemann method

As we saw earlier, Bodvarsson solved the thermal front velocity problem by only considering constant fluid and rock properties. The model consisted of a linear partial differential equation with boundary and initial condition. Stopa and Wajnarowski extended Bodvarsson work to include temperature dependent fluid and rock properties. In this new method, we formulate the problem as a Riemann problem by changing the boundary and initial problem of Bodvarsson and Stoppa and Wajnaroski to an initial problem. By doing so we transform the problem to the well known Riemann problem which is well studied and possess a unique solution. The thermal front velocity is then given by the so called Rankine-Hogoniot copndition

Injecting colder water into a hot geothermal reservoir can be formulated as a Riemann problem : Find the unique weak solution u of

$$\frac{\partial u}{\partial t} + \frac{\partial G(u)}{\partial x} = 0, \quad u(x,0) = g(x) \tag{3.36}$$

$$g(x) = \begin{cases} u_l & \text{if } x \leq 0 \\ u_r & \text{if } x \geq 0\,. \end{cases}$$

satisfying the Rankine-Hugoniot shock condition and the Kruzkov entropy condition [34]. The shock condition gives the speed s of the discontinuity solution of (3.36):

$$s = \frac{G(u_r) - G(u_l)}{u_r - u_l} \tag{3.37}$$

The Kruzkov entropy condition [34]:

$$\int_0^T \int_{-\infty}^{\infty} (\mid u - k \mid \varphi_t + q(u,k)\varphi_x)\,\mathrm{d}x\mathrm{d}t + \int \mid u(x,0) - k \mid \varphi(x,0)\mathrm{d}x \geq 0 \tag{3.38}$$

is the extra condition satisfied by the unique solution of (3.36), where

$$q(u,k) = sign(u,k)(G(u) - G(k)),$$

k is a non negative constant and φ is any non negative test function [34]. The unique solution of (3.36) satisfying the Rankine-Hugoniot condition and the Kruzkov entropy condition is [34].:

$$u(x,t) = \begin{cases} u_l & \text{if } x \leq G'_{\cup}(u_l)t, \\ (G'_{\cup})^{-1}(\frac{x}{t}) & \text{if } G'_{\cup}(u_l)t \leq x \leq G'_{\cup}(u_r)t \\ u_r & \text{if } x \geq G'_{\cup}(u_r)t \end{cases} \tag{3.39}$$

If $u_l < u_r$, and:

$$u(x,t) = \begin{cases} u_l & \text{if } x \leq G'_{\cap}(u_l)t, \\ (G'_{\cap})^{-1}(\frac{x}{t}) & \text{if } G'_{\cap}(u_l)t \leq x \leq G'_{\cap}(u_r)t \\ u_r & \text{if } x \geq G'_{\cap}(u_r)t \end{cases} \tag{3.40}$$

if $u_l > u_r$, where $G_{\cup}$ and $G_{\cap}$ are the lower and the upper convex envelope of G, respectively.

When fluid and rock properties depend continuously on temperature, the flux function G is given by

$$G(u) = V_w \int_0^u F(\theta)\mathrm{d}\theta$$

with

$$F(u) = \frac{\phi\rho_w(u)\left(\frac{\partial(c_w(u)u)}{\partial u}\right)}{(1-\phi)\left(\frac{\partial(\rho_r(u)c_r(u)u)}{\partial u}\right) + \phi\rho_w(u)\left(\frac{\partial(c_w(u)u)}{\partial u}\right)} \tag{3.41}$$

Figure 3.6 shows a general concave energy flux function (left) and its derivative (right). While the energy flux G (left) is general in Figure 3.6, Its derivative F (right) is represented by equation (3.41) as a function of temperature u.

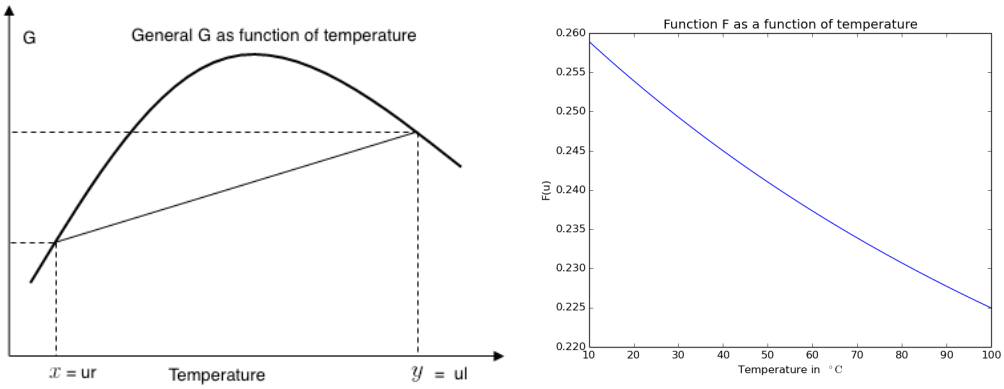

Figure 3.6: The energy flux G (left) and its derivative F (right) with temperature ($x = u_l, y = u_r$). F is given as a function of temperature u in °C

From Figure 3.6, F is monotonically decreasing on the interval $[u_l = 10\,^{\circ}\mathrm{C}, u_r = 100\,^{\circ}\mathrm{C}]$, therefore the flux function G is concave on that interval. The lower convex envelope $G_{\cup}$ of G is the line passing through the points $(u_l, G(u_l))$ and $(u_r, G(u_r))$. In this case the unique solution of equation (3.36) shown in Figure 3.7 moves at the speed $s = V_{TF}$ and is given by

$$u(x,t) = \begin{cases} u_l & \text{if } x \leq st \\ u_r & \text{if } x \geq st \,. \end{cases}$$

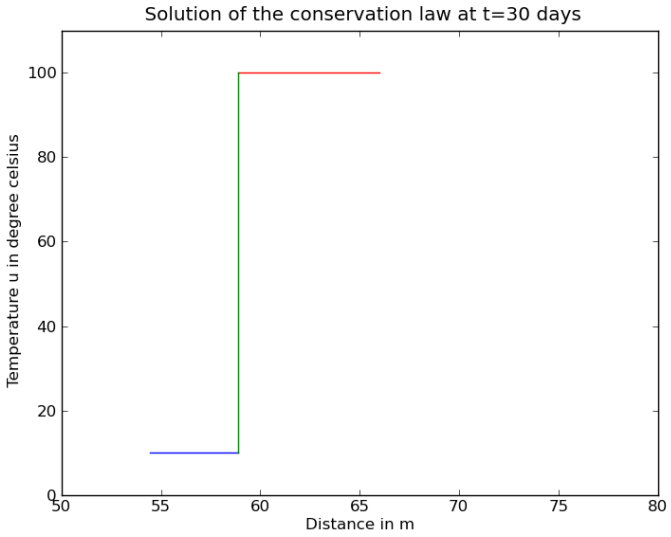

Figure 3.7: Solution of equation (3.36) at t = 30 days. With $u_l = 10\,^{\circ}\mathrm{C}$, $u_r = 100\,^{\circ}\mathrm{C}$

with $s = V_{TF}$ given by the Rankine-Hugoniot shock condition

$$\begin{aligned} s &= v_{TF} \\ &= \frac{G(u_l) - G(u_r)}{u_l - u_r} \\ &= \frac{\frac{u_w}{\phi}}{(u_r - u_l)} \left(\int_0^{u_r} F(u)\mathrm{d}u - \int_0^{u_l} F(u)\mathrm{d}u \right) \\ &= \frac{\frac{u_w}{\phi}}{(u_r - u_l)} \left(\int_0^{u_l} F(u)\mathrm{d}u + \int_{u_l}^{u_r} F(u)\mathrm{d}u - \int_0^{u_l} F(u)\mathrm{d}u \right) \\ &= \frac{1}{(u_r - u_l)} \left(\int_{u_l}^{u_r} \frac{u_w}{\phi} F(u)\mathrm{d}u \right). \end{aligned} \tag{3.42}$$

Figure 3.7 shows the position of the cold injected fluid after 30 days. The injected fluid is at $10\,^{\circ}\mathrm{C}$ initially, while the reservoir is initially at $100\,^{\circ}\mathrm{C}$. The cold injected fluid is represented by the sharp vertical line. In terms of hyperbolic conservation laws, we say that the solution is a shock. Recall that in deriving equation (3.36), conduction which has a smoothening effect on the temperature field was neglected. Therefore in absence of conduction, the temperature filed is discontinuous as seen in Figure 3.7.

3.5 Comparison of the various methods

To evaluate and compare the thermal front velocity obtained in this work and the one obtained in [48], we use the simple yet powerful numerical integration method called the

trapezoidal rule. The trapezoidal rule from elementary calculus states that the integral of a function f on an interval $[a, b]$ subdivided by n mesh points can be approximated by

$$\int_a^b f(x)\mathrm{d}x \approx \frac{b-a}{2n}\left(f(a)+f(b)+2\sum_{i=1}^{n-1} f(a+ih)\right) \tag{3.43}$$

with absolute and asymptotic error (computable error) given respectively by

$$E_n^a = -\frac{h^2(b-a)}{12}(f''(c_n)) \tag{3.44}$$

and

$$E_n^c = -\frac{h^2}{12}(f'(b)-f'(a)) \tag{3.45}$$

with some unknown $c_n \in [a, b]$ and $h = \frac{b-a}{n}$. Equation (3.45) is also called upper bound error and can also be written in terms of n as

$$E_n^c = \frac{c}{n^2} \tag{3.46}$$

with

$$c = -\frac{(b-a)}{12}(f'(b)-f'(a)).$$

To evaluate the derivative of f we use the finite difference approximation

$$f'(x) \approx \frac{f(x+h)-f(x-h)}{2h}$$

with approximation error given by

$$Err = \frac{1}{6}f'''h^2 + O(h^3) = O(h^2). \tag{3.47}$$

Let recall here the different models for the thermal front velocity obtained by Bodvarsson, Stopa and Wajnarowski and the Riemann method, repectively:

$$V_1 = \left(\frac{u_w}{\phi}\frac{\phi\rho_w c_w}{(1-\phi)\rho_r c_r + \phi\rho_w c_w}\right) \tag{3.48}$$

$$V_2 = \frac{u_w}{\phi}\left(\frac{\int_{u_l}^{u_r} U(u)F(u)\mathrm{d}u}{\int_{u_l}^{u_r} U(u)\mathrm{d}u}\right) \tag{3.49}$$

$$V_3 = \frac{1}{(u_r-u_l)}\left(\int_{u_l}^{u_r}\frac{u_w}{\phi}F(u)\mathrm{d}u\right) \tag{3.50}$$

By using the trapezoidal rule (3.43), we evaluate equation (3.50) derived in this work and equation (3.48) from [48], to approximate the thermal front velocity. Table 3.2 compares the values of the thermal front velocity obtain in [48] and the one predicted by the theory of conservation laws presented in this work. Table 3.3 shows the thermal front velocity obtained from Bodvarsson, for constant fluid and rock properties. The thermal front veloc-

Table 3.2: Approximated values for evaluating (3.50) from this work and (3.49) from [48], with $\phi = 0.15$, $u_w = 10^{-4} m/s$

u_l (°C)	u_r (°C)	$V_3\ (m/s)$	$V_2\ (m/s)$	$V_3 - V_2\ (m/s)$
10	100	2.261×10^{-5}	2.257×10^{-5}	$4 * 10^{-8}$
55	100	2.15×10^{-5}	2.15×10^{-5}	0.0
10	55	2.370×10^{-5}	2.369×10^{-5}	10^{-8}
20	80	2.271×10^{-5}	2.269×10^{-5}	$2 * 10^{-8}$
30	70	2.264×10^{-5}	2.263×10^{-5}	10^{-8}
40	60	2.260×10^{-5}	2.259×10^{-5}	10^{-8}

Table 3.3: Fluid and rock properties used for computing V_1 with $\phi = 0.15$, $u_w = 10^{-4} m/s$

Temperature (°C)	$c_r\ (J/Kg.°C)$	$c_w\ (J/Kg.°C)$	$\rho_r\ (Kg/m^3)$	$\rho_w\ (Kg/m^3)$	V_1 (m/s)
100	928.75	4210	2639	957.57	1.499×10^{-4}
80	903	4187	2643	968.6	1.594×10^{-4}
70	890	4180	2642	973.57	1.559×10^{-4}
60	876	4176	2644.7	978	1.582×10^{-4}
55	868.94	4175	2645	980	1.594×10^{-4}

ity predicted by the theory of conservation laws is slightly higher than the one obtained by Stopa and Wajnaroski in [48]. A relative error of 10^{-3} is observed between the two results. The thermal front velocity from Bodvarsson given by equation (3.48) is on average six times larger then the one predicted by Stopa and Wajnaroski from equation (3.49) and the Riemann method given by equation (3.50). It can therefore be seen as the worst case scenario. This suggests that temperature dependent fluid and rock properties act as a damping mechanism on the thermal front velocity.

From equation (3.46) we see that the trapezoidal rule is second order accurate and the computed convergence rate p can be computed by rewriting equation (3.46) in terms of p as

$$E_n^c = \frac{c}{n^p}. \tag{3.51}$$

By taking the log of equation (3.51) and rearranging the terms we get

$$p = \frac{\ln(E_{n-1}/E_n)}{\ln(n/n-1)} \tag{3.52}$$

where n is the number of subdivision of the interval $[a, b]$ and E_n is the corresponding error given by equation (3.45). Table 3.4 shows that the computed convergence rate is approximately equal to the theoretical convergence rate $p = 2$. This shows that the numerical approximations performed by using the trapezoidal rule are accurate. The importance of the analytical method presented in this work can be express as follow: given a geothermal reservoir with temperature u_r and injected fluid temperature u_l, and assuming that 100% of the injected fluid reach the production well, the thermal front velocity can be computed and the thermal breakthrough time can thus be approximated. Since a geothermal system properties

Table 3.4: Convergence rate for the the trapezoidal rule

n	E (10^{-6})	convergence rate p
4	351	1.99
5	225	2.01
6	156	1.98
7	115	

such as heat capacity and density are temperature dependent, the thermal front velocity depends only implicitly on temperature. The thermal front velocity models presented in this Chapter is conservative. Meaning that the models assume 100 $\%$ fluid recovery at the injection well. In practice only a fraction of the injected fluid is recovered at the injection well. It is therefore recommended to perform a tracer test to estimate the thermal front velocity.

The models presented in this work are only one dimensional. The temperature dependent case can be extended to two or even three dimensions from the theory of hyperbolic conservation laws as

$$\frac{\partial u}{\partial t} + \nabla \mathbf{G} = \frac{\partial u}{\partial t} + \frac{\partial G_x}{\partial x} + \frac{\partial G_y}{\partial y} + \frac{\partial G_z}{\partial z} \tag{3.53}$$

where G_x, G_y, G_z are the x, y and z components, respectively of the energy flux $\mathbf{G}$ which is now a vector. The advantage of the Riemann method over the one developed by Stopa and Wajnarowski is that multi dimensional conservation laws such as equation (3.53) are well studied and there are numerous numerical methods available to treat this problem. In addition, the Riemann method only requires the injected fluid temperature, the reservoir temperature and the energy flux which is defined in the governing equation. No additional parameter is needed. In the method proposed by Stopa and Wajnarowski, the internal energy of the system need to be computed. Conservation of energy can be difficult to implement in three dimensions. Therefore the Riemann method is easily scalable as opposed to the method proposed by Stopa and Wajnarowski.

Chapter 4

Lumped parameter modelling

4.1 Lumped parameter modelling

The lumped parameter modelling implementation in this work was introduced by Axelsson [5]. It is an inverse modelling method, applied successfully to simulate pressure response data, and assess global hydrological characteristics in low temperature geothermal reservoir in Iceland, and in many geothermal system around the world [5]. It is a cost effective and reliable alternative to detail numerical modelling which can be time consuming, costly and requiring large amount of data [5]. Lumped parameter modeling provides the first step when evaluating production data from a liquid dominated geothermal system [31]. It also can indicate whether the main production mechanism is confined or unconfined [31].

The application of lumped parameter models for interpreting geophysical data was pointed out by Bodvarsson [5, 16]. The method has been applied to model diverse geothermal reservoirs: Wairakei in New Zealand [47, 52], Svartsengi in Iceland [31, 30, 35], Larderello in Italy [19], to cite but few. In the lumped model, the geothermal system is represented by tanks, characterised by storage coefficient κ, with conductor σ, simulating respectively the storativity s and permeability k. In this modelling process the reservoir is divided into 1-3 parts if necessary, as shown in Figure 4.1. For two dimensional flow as in this work, the fluid turbulence coefficient is neglected. Each part is approximated by a cylindrical tank with defined radius as shown in Figure 4.1. The innermost cylinder (inner tank) is the production part which is intersected by the production well. Adjacent to the innermost cylinder is an

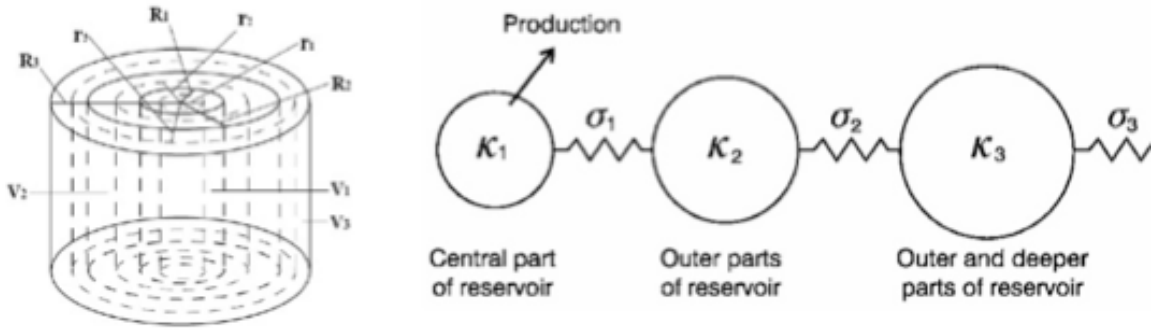

Figure 4.1: Subdivision of the reservoir in recharge, intermediary, and production parts for lumped parameter modelling

intermediate cylinder defining the interface between the recharge part (outer cylinder) and the production part (innermost cylinder). Each cylinder is then approximated by a lumped capacitor characterised by the coefficients κ and σ simulating storativity s and permeability k respectively, of the cylinder (capacitor) and the region connecting cylinders.

4.2 Mathematical formulation

The theoretical background of the lumped parameter modelling discuss in this section is entirely taken from [1, 5]. The lumped parameter modelling approach is very convenient due to the simple mathematical relation between the elements. In this approach, the elements are connected in a network with explicit mathematical relations derived from the physics of the entire network. Consider N linear time independent capacitors with capacitance κ_j represented in Figure 4.2. Each capacitor can be represented by a cylinder with sufficient depth. It is assumed that the cylinder depth is such that it can not be empty by any flow process. The pressure P of the capacitor is

$$P = \frac{m}{\kappa}$$

where m is the mass of the liquid contained by the capacitor with capacitance κ. The conductance between conductor i and k is σ_{ik} and by linearity

$$\sigma_{ik} = \sigma_{ki}, \quad \sigma_{ii} = 0.$$

The network is open such that the ith capacitor is connected by a conductor of conductance σ_i to an external capacitor at an equilibrium pressure ($P = 0$). The network is closed when $\sigma_i = 0$ for $i = 0, 1, 2, \cdots$. The mass flow q_{ij} between conductor i and k at pressures P_k and P_i is given by

$$q_{ik} = \sigma_{ik}(P_k - P_i). \tag{4.1}$$

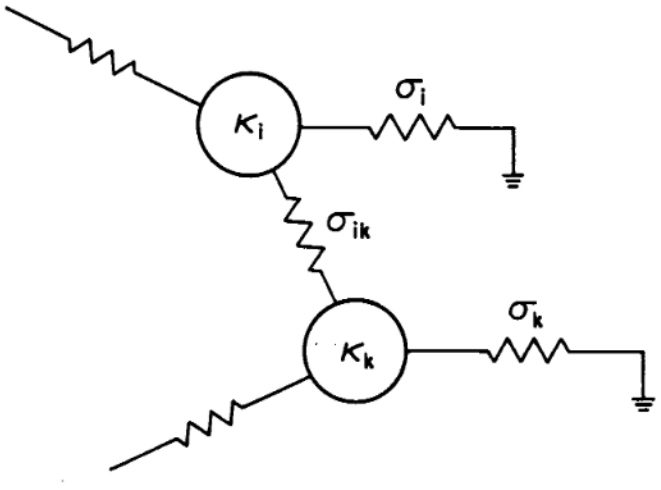

Figure 4.2: General configuration of the network of capacitors

The conservation of mass for the network can be formulated as

$$\kappa_i \frac{dP_i}{dt} = \sum_{k=1}^{N} (q_{ik} - \sigma_i P_i + f_i) \tag{4.2}$$

where f_i is an external source force on element i. The basic system of equations for the entire network derive by inserting equation (4.1) into equation (4.2) is:

$$\kappa_i \frac{dP_i}{dt} = \sum_{k=1}^{N} \left(\sigma_{ik} P_k - P_i \left(\sum_{k=1}^{N} (\sigma_{ik} + \sigma_i) \right) + f_i \right) \tag{4.3}$$

with a corresponding matrix formulation

$$\mathbf{k} \frac{d\overline{P}}{dt} + \mathbf{A}\overline{P} = \overline{f}, \tag{4.4}$$

where

$$\overline{P} = (P_i)$$
$$\overline{f} = (f_i)$$
$$\mathbf{k} = [\kappa_i \sigma_{ik}]$$

$$\mathbf{A} = \left[\left(\sum_j \sigma_{ij} + \sigma_i \right) \sigma_{ik} - \sigma_{ik} \right]$$

4.3 Solution procedure and implementation

If the network is subjected to a general force $\overline{f}(t)$ and is taken to be at equilibrium, the response of the network is

$$P(t) = \sum_{k=0}^{N} \left\{ \int_0^t \overline{h}_k(t-\tau) f_k(\tau) \mathrm{d}\tau U_+(\tau) \right\},$$

where $\overline{h}_k$ is the response of the network to an impulse force

$$\overline{f}(t) = \overline{\Delta}_k \delta_+(t),$$

satisfying

$$\mathbf{k} \frac{d\overline{h}_k}{dt} + \mathbf{A}\overline{h}_k = \overline{\Delta}_k \delta_+(t), \tag{4.6}$$

where $\overline{\Delta}_k$ is the vector with non vanishing component equal to unity at entry k. The solution of equation (4.6) by operational calculus is

$$\overline{h}_k = \exp\{-t\mathbf{R}\} k^{-1} \overline{\Delta}_k U_+(t),$$

where the decay rate matrix $\mathbf{R}$ is given by

$$\mathbf{R} = k^{-1}\mathbf{A} \tag{4.7}$$

If f is a step function rather than a pulse function as before, the response of the network subjected to mass flow equal $q_k U_+(t)$ from conductor k is given by

$$P_{ik}(t) = q_k U_+(t) \sum_{j=1}^{N} \left(\frac{\tau_{ij}\tau_{kj}}{\lambda_j}(1 - e^{-\lambda_j t}) \right) \tag{4.8}$$

where $\lambda_j, \overline{\tau}_j$ are respectively the eigenvalues and eigenvectors corresponding to the solution of the eigenvalue problem

$$\mathbf{A}\overline{\tau} = \lambda k \overline{\tau} \tag{4.9}$$

or

$$\mathbf{R}\overline{\tau} = \lambda \overline{\tau}, \tag{4.10}$$

where R is given by equation (4.7). The matrix **A** is a real matrix for an open system and a real singular matrix for a closed system. The orthogonality relation for the eigenvector is

$$k(\overline{\tau_i}, \overline{\tau_k}) = \delta_{ij}$$

where the Dirac delta function is given by

$$\delta_{ij} = \begin{cases} 1 & \text{if } i \neq j \\ 0 & \text{if } i = j \end{cases}$$

In the next section, lumped parameter modelling is used to model the water level of a low temperature geothermal system. The mathematical equations were implemented in the generic software LUMPFIT developed by Axelsson [1]. By using a nonlinear iterative least square technique, the computer program LUMPFIT fits automatically the analytical response functions of lumped models to the measured data (water level or pressure) [5]. The equations used in LUMPFIT are

$$P(t) = \sum Q \frac{A_i}{L_i}(1 - exp(-L_i t))_{i=1}^{N-1} + QBt \tag{4.11}$$

for an closed system, and

$$P(t) = \sum Q \frac{A_i}{L_i}(1 - exp(-L_i t))_{i=1}^{N-1}. \tag{4.12}$$

for a open system. The relationship between pressure and water level is given by

$$P(t) = \rho g h(t) \tag{4.13}$$

The parameters A_i, L_i, B, are function of κ_i and σ_i. After evaluating the unknown parameters (A_i, L_i, B, κ_i and σ_i), equations (4.11, 4.12) can be used to simulate and predict water level change in time. The size A, the depth H, the approximate permeability k, the storativity s and the recharge mechanism of the reservoir can also be evaluated and understood using:

$$\kappa_i = V_i s = A_i H s \tag{4.14}$$

$$k = \sigma_i \frac{ln(r_{i+1}/r_i)\nu}{2\pi H} \tag{4.15}$$

$$r_1 = R_1/2, \quad r_2 = R_1 + (R_2 - R_1)/2, \quad r_3 = R_2 + (R_3 - R_2)/2 \tag{4.16}$$

$$R_1 = \sqrt{V_1/\pi H}, \quad R_2 = \sqrt{(V_1 + V_2)/\pi H}, \quad R_3 = \sqrt{(V_1 + V_2 + V_3)/\pi H} \tag{4.17}$$

Lumped parameter modelling is applied in the later chapter to a case study. The case satudy is consern with determining important parameters of the geothermal system, such as reservoir size, permeability and storage mechanism among others.

Chapter 5

Case study: Munadarnes low temperature geothermal system

5.1 The Munadarnes low temperature system

The Munadanes geothermal reservoir is situated in the Nordurardalur geothermal field, see Figure 5.1. The latter is located in west Iceland in the Borgarfjordur geothermal region situated in Borgarfjordur. The Borgarfjordur thermal region shown in Figure 5.1 is amongst the largest low temperature geothermal regions in Iceland. It comprises known thermal systems such as the Reykholtsdalur thermal system, the Baer thermal system, the Brautartunga thermal system, England thermal system, the Husafell thermal system and also the Nordurardalur geothermal system (Johannesson et al. 1980, Gunnlaugsson 1980). The natural discharge of the Reykholtsdalur thermal system is estimated to be $450 l/s$ of boiling water (Georgsson et al. 1984). Within the Borgarfjordur thermal region, the Reykholtsdalur thermal system is by far the largest thermal system with a total discharge of $400 l/s$ (Georgsson

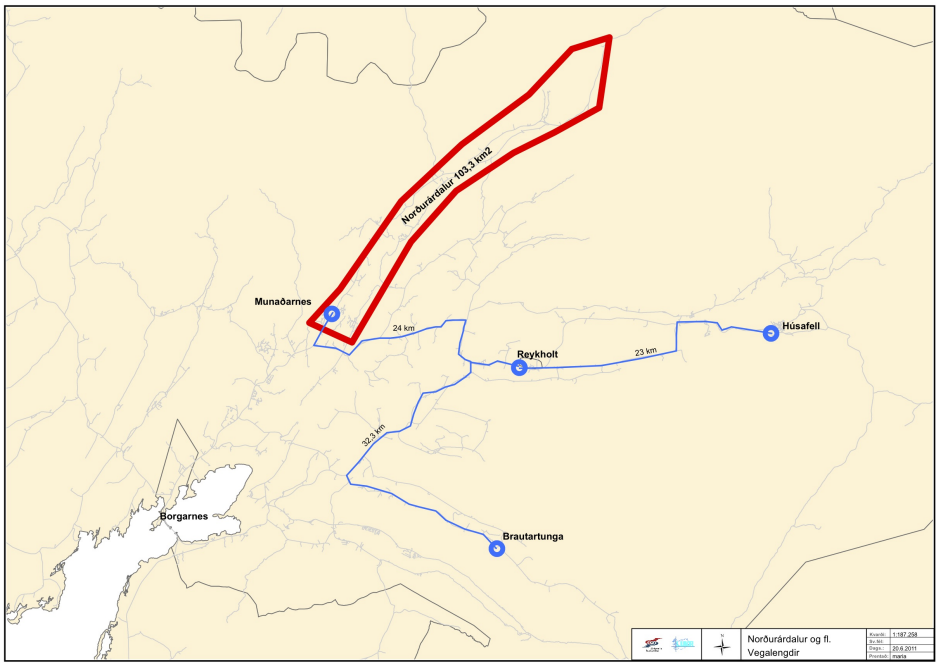

Figure 5.1: Borgarfjordur thermal region and the Nordurardalur geothermal system

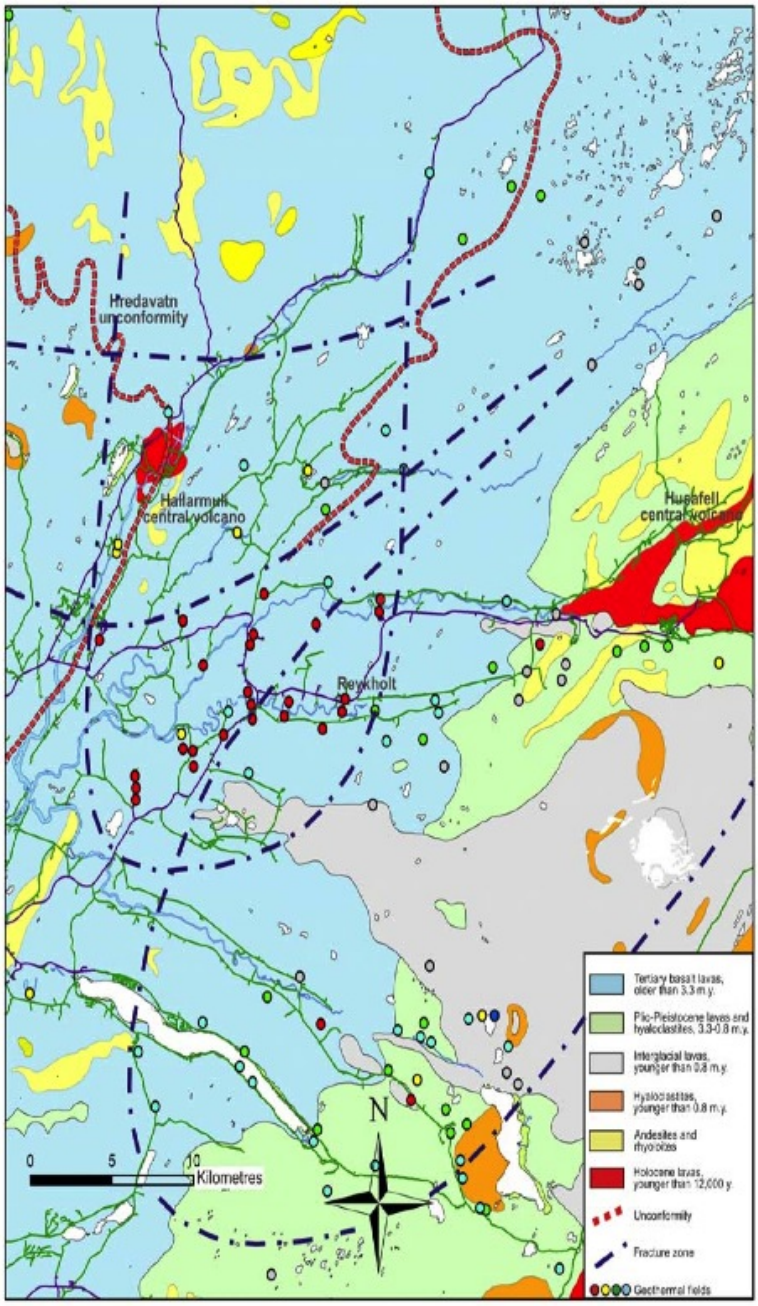

Figure 5.2: Geological map of Borgarfjordur thermal region, taken from [28]

et al. 1980). The Nordurardalur thermal system is located north-west of the five major thermals systems mention above. It constitutes a N-W long band of about 103 km^2 .

5.1.1 Geological setting

Upper tertiary (>3.3 Myr) basaltic lava flows constitute the basement of the Borgarfjordur region. These lava flow are characterised by a uniform lithology, either uniform texture or composition, the oldest rock being 14-15 Myrs. The bulk of these tertiary lava flows is made of tholeiites basaltic rock separated by minor clastic interbeds (Saemundsson, 1979). The tholeiitic basaltic lava pile is characterized by its content in sodium which is less than other basaltic rock. The Borgarfjordur thermal field is bounded on the east by the western vol-

canic rift zone and the Snaefellnes volcanic zone from the west. The latter presents little or no rifting. These two volcanic zones represent the origin of the tertiary lava flows. However, the tholeiitic content of the lava flow suggests that the lava flow is predominantly from the Sneafellsnes volcanic flank zone.

Both unconformity and anticline structures are visible in the region. The latter resulted from rift relocation (Saemundsson, 1967). Recall that an anticline is defined as layers of rock having the oldest strata in its core and forming a convex shape. An unconformity is a planar structure indicating a discontinuity in a geological structure due to erosive forces. The anticline axis is defined as the line of intersection of the perpendicular plane cutting the anticline in two symmetric parts. The Borganes anticline runs NE-SW (Saemundsson, 1977). The lava flows dips towards the Reykjanes-Langjokull rift zone to the east of the anticline axis. The Hredavatn unconformity shown in Figure 5.2 is situated north of Hredavatn lake. This unconformity indicates intense erosive forces acting in the Borgarfjordur region.

5.1.2 Geophysical and hydrological setting

The geophysics of the region is characterised by the volcanism, the tectonic setting and the different forces affecting the crustal structure. The region is located between the Sneafellsnes volcanic flank and the Reykjanes-Langjokull volcanic rift. The latter includes the Reykjanes peninsula and the Western volcanic zone. The Reykjanes-Lanjokull rift is characterised by faulting resulting from tensional stress in the earth crust. The Nordurardalur geothermal system is confined within the WNW-ESE, N-S fractures zone and between the Hradavatn unconformity and the Borganes anticline.

The resistivity survey in Nordurardalur alternates between 20 and 100 Ωm. The 20 Ωm resistivity part is located in the lowest part of the Nordurardalur band and it quickly increases to 60 and 100 Ωm as we move northeast. The values alternates to 30-40 Ωm then decrease to 20 Ωm before increasing to about 30 Ωm.

The geothermal water is of meteoric origin and has fallen as precipitation on the highlands around Nordurardalur. The water percolates through fractured, cracks or others pathways through the earth and is heated by regional heat flow. The flow pattern can be inferred base on previous studies done in the main thermal systems in Borgafjordur. The Northeasterly faults are the main channels for the Nordurardalur thermal system and the seismicity in the region allows fractures to serve as flow paths. The recharge zone is the Arnarvatnsheidi highland.

5.1.3 Proposed conceptual model of Borgarfjordur thermal region

Figure 5.3 indicates the flow patterns of the main geothermal systems in the Borgarfjordur thermal region [28]. The Reykholt and the Brautartungar thermal field recharge zone is located in the Arnarvatnsheidi highland. The Husafell thermal system recharge zone is located east of the Arnarvatnsheidi highland. For those three systems, the easterly and northeasterly faults and fractures allow the meteoric water to percolate at depth, acting as flow channels. The Nordurardalur system can be seen as a part of the Baer thermal system [28]. The recharge zone is situated in the highlands around Snjofjoll, latitude 64 ° 59 ' N, longitude 21 ° 11 ' W. The NS fractures act as flow channels, where the water flows by the Hallarmuli extinct central volcanoe.

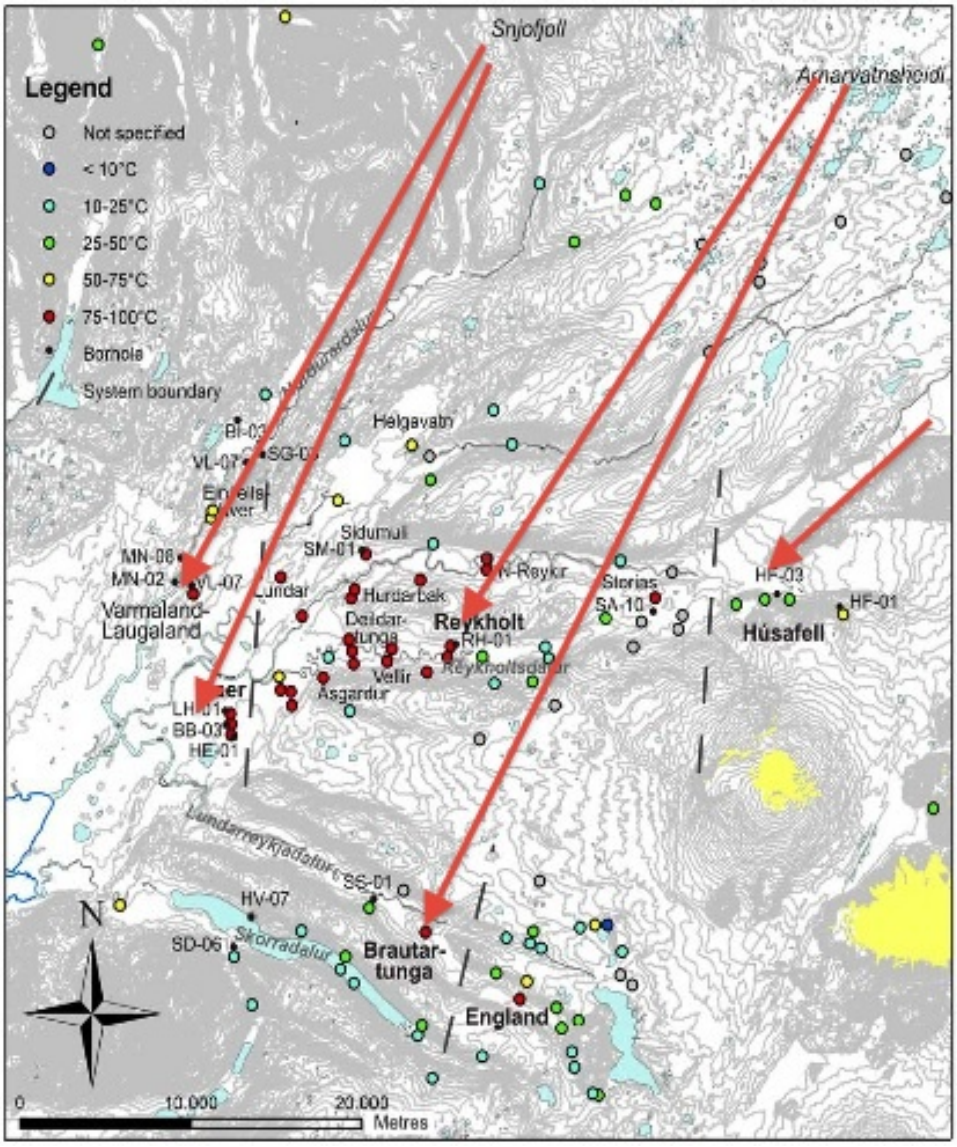

Figure 5.3: Production wells in Borgarfjordur thermal field with proposed flow patterns of the main thermal systems, taken from [28]

Heat is transferred by conduction through the Earth's crust from the Snaefellsnes volcanic flank zone and the Reykjaness-Langjokull volcanic rift zone. Heat is convected by the hot water though the fracture and fault systems at depth. The thermal energy comes also from depth. The thermal energy transferred by the geothermal activity also comes from stored energy around the fractures, generally in the crust, specifically in extinct central volcanoes.

The integrity of the fracture/fault systems is maintain by the seismicity in the region. Some fractures/faults also act as barrier zones. The salinity of water is the highest in the Baer thermal system as well as in the Nordurardalur system. As we move away from the Baer system the salinity decreases, being the lowest in Husafell thermal system.

5.2 Lumped parameter modelling of well $MN08$ in Munadarnes

Well $MN08$ was drilled in 2003 east of the summer house located in Munardanes. The $900m$ deep low temperature well owned by Reykjavik Energy was drilled after a survey revealed a temperature gradient of $250\,^{\circ}\mathrm{C}/km$ [45]. The convective part starts at 430-450 m judging from the temperature profile and probably extends deeper than the bottom of the well. According to the temperature measurement the thickness, H, of the reservoir is at least 450 m but is assumed 900 m in this case. Testing and measurement of the well from February to March 2003 revealed that the temperature of the well is approximate $90\,^{\circ}\mathrm{C}$ and the main feed zone is located at about $440m$ depth [45]. Figure 5.4 shows temperature measurement in well $MN08$ in 2003 while Figure 5.5 shows temperature measured in well $MN08$ from January 2008 to October 2010. Water level, pressure, temperature and production rate have been monitored for the well since January 2008 with data up to December 2010 available for this study. The well was drilled in 2003 with an initial water level of $35m$. The data set was rearrange by eliminating outliers, that is data points that are numerically distant from the rest of the data, most likely because of measurement errors. The new data set was however still spread out. The data consisted of water level measurement in m, with corresponding production rate in l/s and measurement date. The problem at hands can be formulated as follows: given the set of data, find the physical parameters such as permeability, storativity and determine the storage mechanism of the reservoir intersecting well $MN08$. The problem is well explain by the flowchart below:

This is an inverse problem: fitting the models given by equations (4.11), (4.12) and (4.13) to data represented by water level, production rate and date, to find reasonable values for the parameters such as permeability, storativity and ultimately determine the storage mechanism of the reservoir intersecting well $MN08$ in Munadarnes. The solution of this problem is provided by the software LUMPFIT which uses a non-linear iterative least square technique to simulate the data. Figure 5.6 shows the original water, from January 2008 to December 2010, while Figure 5.7 shows the production rate measured in well $MN08$ from January 2008 to October 2010. Despite the spreading of the data, a satisfactory two tank open model was obtained and later used for future predictions. Figure 5.8 shows the water level without

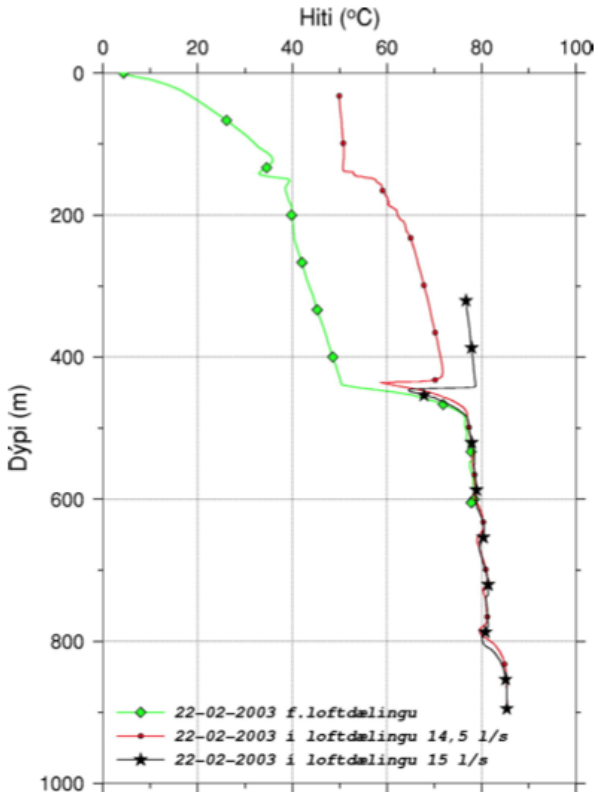

Figure 5.4: Temperature measurement in well $MN08$ in 2003, taken from [45]

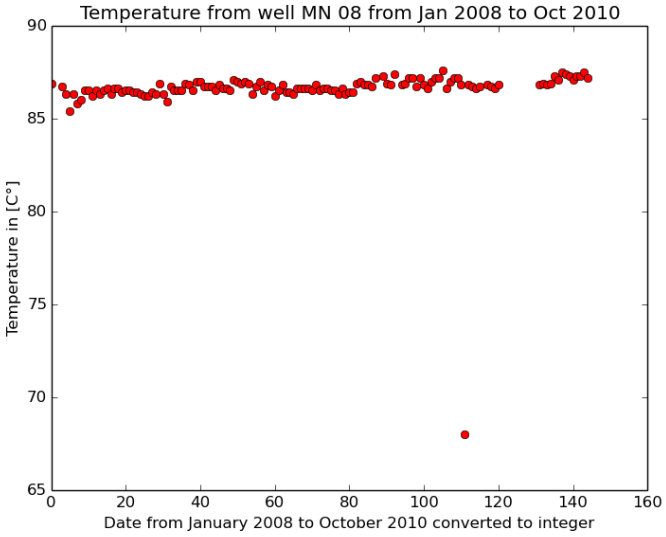

Figure 5.5: Temperature measurement in well $MN08$ from January 2008 to October 2010

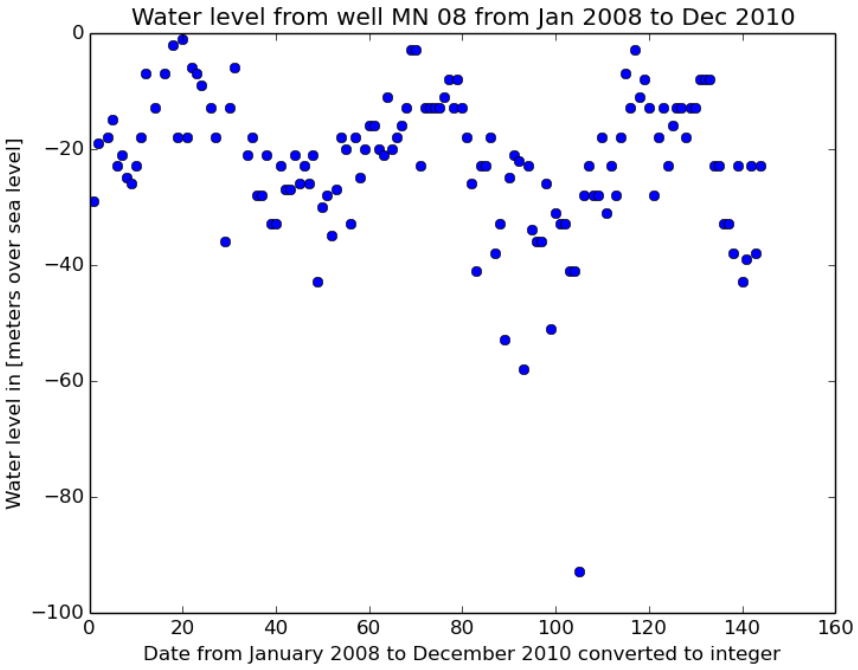

Figure 5.6: Water level measured in well $MN08$ from January 2008 to December 2010

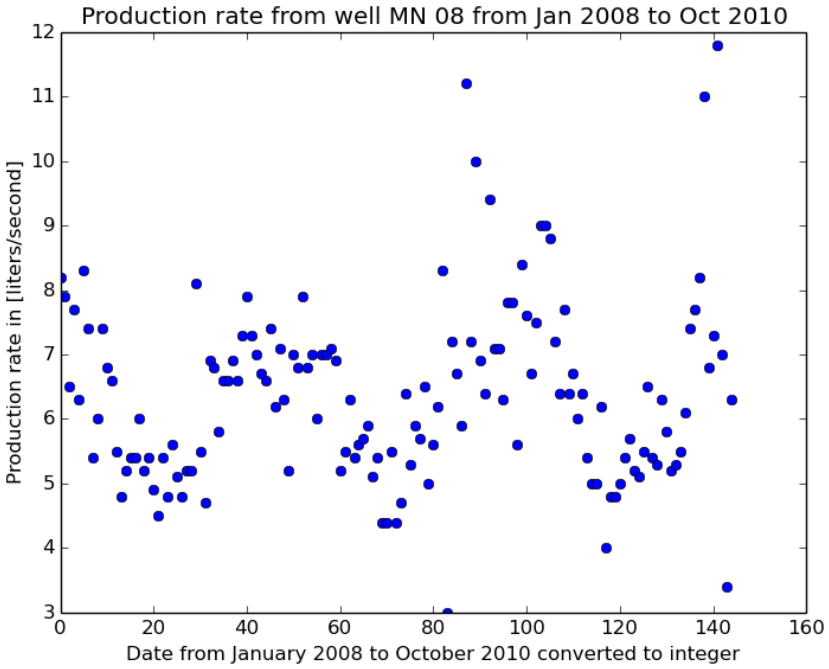

Figure 5.7: Production rate measured in well $MN08$ from January 2008 to October 2010

outliers and the simulation result from LUMPFIT with two tank open model from January 2008 to December 2010. Table 5.1 shows the estimation of the physical parameters obtained from simulating water level and production rate over a period of three years. In Table 5.2, the storativity of a confined (s_c) and an unconfined (s) reservoir are estimated based on the parameters computed. From the simulation we can infer the storage mechanism of

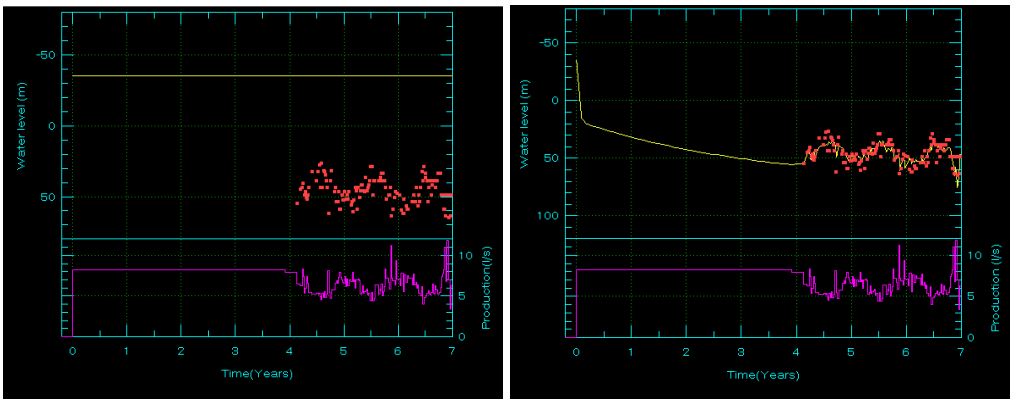

Figure 5.8: Two tank open model LUMPFIT simulation result of water level data from well $MN08$, from Jan 2008 to December 2010. Left: initial water level before simulation, right:simulation result from LUMFIT.

Table 5.1: Parameters of the lumped models for the production well $MN08$ in Munardanes

Model number	1	2	3	4
Number of tanks	1	1	2	2
Number of parameters	2	4	6	8
Model types	Closed	Open	Closed	Open
A_1	0	10.14	10.85	17.8979
L_1	0	0.8	1.16	2.82
A_2	0	0	0	0.17
L_2	0	0	0	0.025
B (10^{-3})	154.4	0	41.3	0
κ_1	1741.4	26.52	24.68	14.88
κ_2	0	0	6487.2	1593.36
κ_3	0	0	0	0
$\sigma_1(10^{-6})$	0	8	10.83	16.8
$\sigma_2(10^{-6})$	0	0	0	15.2
$RMS(m)$	12.26	7.46	6.65	5.91
$STD(m)$	12.31	7.52	6.73	6.01
$R^2(\%)$	0.00	30.6	44.88	56.46

Table 5.2: Storativity estimation for well $MN08$ in Munardanes. s is the storativity of a unconfined reservoir while s_c is the storativity of a confined reservoir.

Porosity ϕ	0.15
depth $H(m)$	900
gravity (m/s^{-2})	9.81
Water compressibility $C_w(10^{-10}Pa^{-1})$	4.6534
Rock compressibility $C_r(10^{-10}Pa^{-1})$	3.3
$s_c(10^{-7}kg/m^3Pa)$	3.4
$s(10^{-5}kg/m^3Pa)$	1.7

the reservoir as follows: If the reservoir was confined and storage controlled by compressibility only, it would cover an area of about $525.5km^2$ which is too large compared to the geothermal field. On the other hand, in the unconfined case (free surface), the total area for the reservoir is about $10.5km^2$. We therefore conclude that the reservoir is unconfined, with an area of approximately $10.5km^2$. The reservoir permeability is estimated at about $70\ mDarcy$ assuming a depth of 900 m. The Borgarfjodur thermal region is estimated at $300Km^2$ and is the largest low-temperature in Iceland, but most of the upflow is limited to $100Km^2$ [36, 28].

5.2.1 Water level prediction scenario with and without injection

From table 5.1 and equation (4.12) the pressure response and the water level of well MN08 for constant production Q are given respectively by

$$P(t) = Q\left(\frac{17.8979}{2.82}\left(1 - e^{-2.82t}\right) + \frac{0.17}{0.025}\left(1 - e^{-0.025t}\right)\right) \tag{5.1}$$

$$h(t) = \frac{Q}{\rho g}\left(\frac{17.8979}{2.82}\left(1 - e^{-2.82t}\right) + \frac{0.17}{0.025}\left(1 - e^{-0.025t}\right)\right) \tag{5.2}$$

Base on these, a 20 years future prediction is given for 12 different production scenarios below:

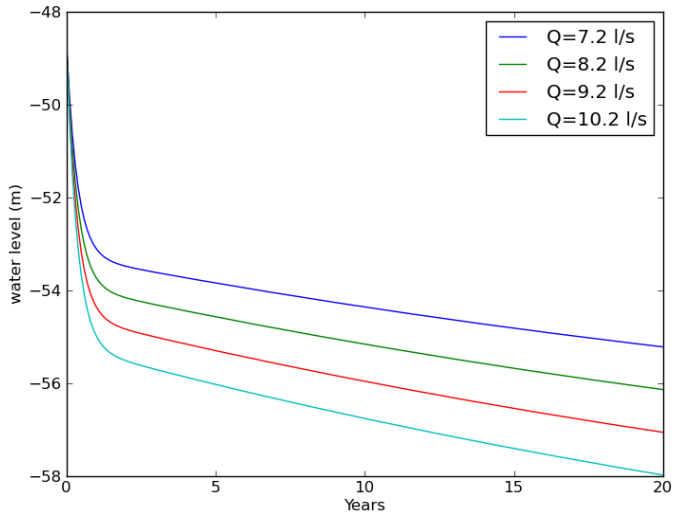

Figure 5.9: 20 years future water level prediction for well $MN08$ from 2010 for 4 scenarios, without reinjection

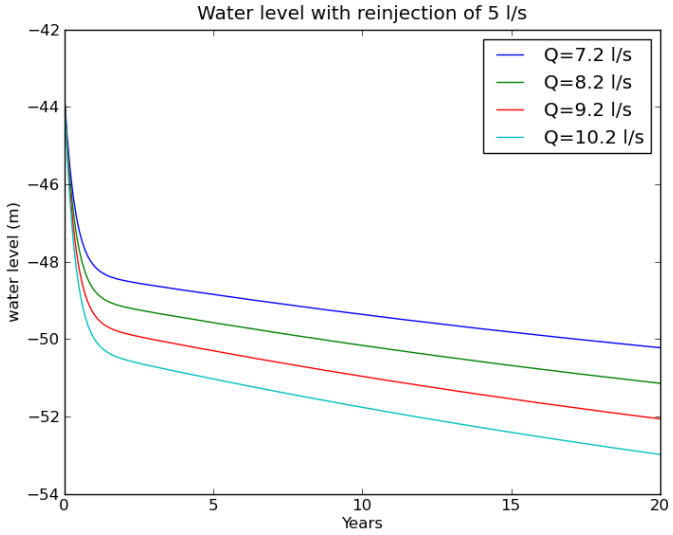

Figure 5.10: 20 years future water level prediction for well $MN08$ from 2010 with reinjection for 4 scenario with 5 l/s injection rate at the start of production

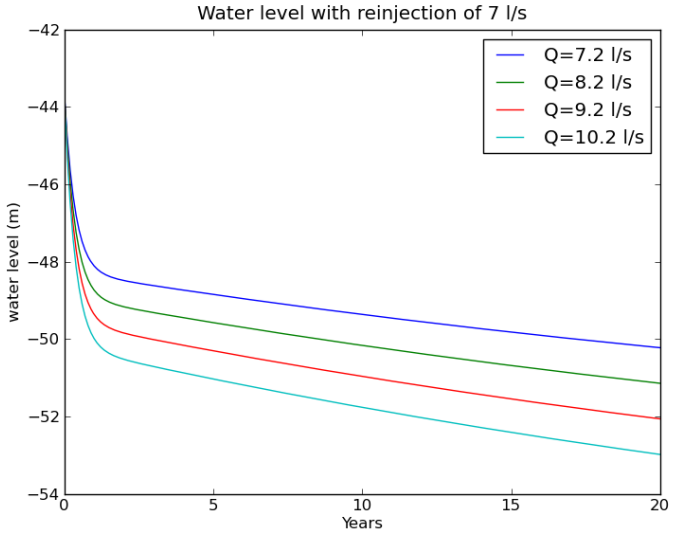

Figure 5.11: 20 years water level prediction for well $MN08$ from 2010 with reinjection for 4 scenario with 7 l/s injection rate at the start of production

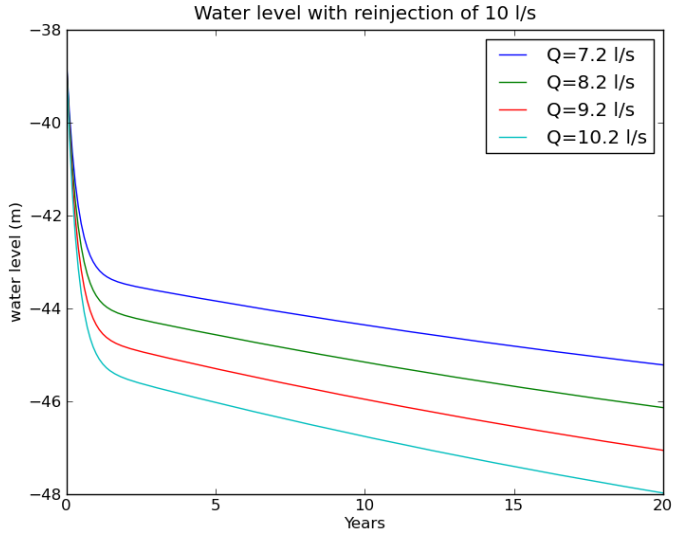

Figure 5.12: 20 years water level prediction for well $MN08$ from 2010 with reinjection for 4 scenario with 10 l/s injection rate at the start of production

Figure 5.9 shows 20 years predictions with production rate of 7.2 l/s, 8.2 l/s, 9.2 l/s and 10.2 l/s. Figure 5.10, 5.11 and 5.12 shows the change in water level over a period of 20 years with three injection scenarios of water at 5, 7 and 10 l/s reinjection rate. The reinjection scenarios assume that reinjection started at the beginning of 2004. The minimum and maximum production rate are assumed to be 7.2 l/s, 10.2 l/s respectively. As seen water level increases significantly with injection.

5.2.2 Temperature field prediction scenario with injection

In this section we compare the results of two models describing the cooling of a low geothermal system due to injection of cold water by applying them to the Munadarnes system.

5.2.2.1 Thermal cooling with conduction

In the first model, based on a theoretical model of a one dimension flow channel (see Figure 5.13), along a fracture zone, the temperature of a production well located at a distance x from an injection well is given by [7]:

$$T(x,t) = T_0 - \frac{q}{Q}(T_0 - T_i)\left(1 - \left(\frac{\lambda x h}{c_w q\sqrt{\lambda(t - x\beta)}}\right)\right) \tag{5.3}$$

Here $T(x,t)$ is the production fluid temperature as a function of position and time, T_0 is the undisturbed reservoir temperature while T_i is the temperature of the injected fluid, q and Q are the rate of injection and production, respectively, λ the thermal conduction of the reservoir rock, κ the thermal diffusivity, x the distance between injection and production wells and t is time. Other parameters in (5.3) are:

$$\beta = \frac{qc_w}{< \rho c >_f \; hb}$$

with

$$< \rho c >_f = \rho_w c_w + \rho_r c_r (1 - \phi)$$

the volumetric heat capacity of the material in the flow channel of width h and height b. The parameters ρ and c are density and heat capacity, respectively, with indices w and r standing for water and rock. Equation (5.3) is valid for

$$t > \frac{x}{\beta} \tag{5.4}$$

Equation (5.3) is the solution of a model where conduction is dominant. Here the thermal conduction coefficient λ shows that conduction is the main mode of heat transfer. Figure 5.13 represents a one dimensional fracture zone with length x, width h and height b. The injected fluid moves through the fracture zone with mass flow rate q. Since the injected water is colder than the surrounding rock, heat will be transferred by conduction from the

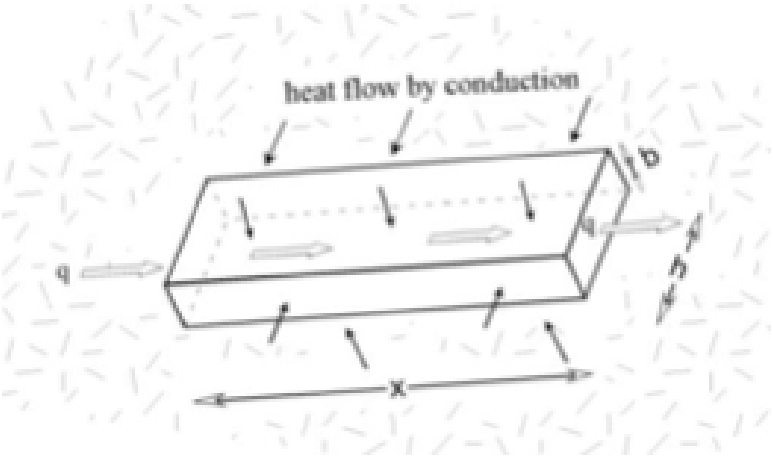

Figure 5.13: Model of flow channel of width h and height b for cooling of production well during injection [7]

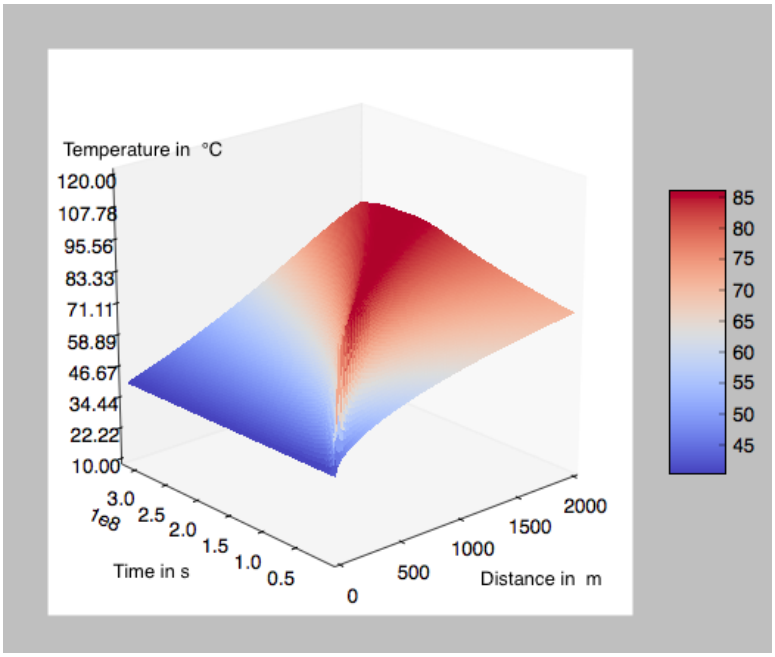

Figure 5.14: 2D graphical representation of equation (5.3). The vertical axis is temperature in °C. The axis in the plane represent distance (0 to 2000 m) and time (0 to 3 years), respectively. The parameters of fracture zone are: $\lambda = 2W/(m \cdot K)$), $h = 40m$, $b = 27m$, $\phi = 0.15$.

rock to the fluid. The temperature profile given by equation (5.3) is therefore the solution of the convection diffusion equation. The diffusion effect represented by conduction has a damping or smoothening effect on the temperature field. This can be seen in Figure 5.14 which represents the temperature profile of a production well fluid in fracture zone, as a function of distance and time from the injection well. As we move away from the injection well toward the production well the injected fluid is heated by the hot rock. Assuming that there is a heat source, we will observe an increase in the injected water temperature as it moves from the injection well.

Assume a one dimensional channel with $h = 40\ m$, $b = 27\ m$ and porosity $\phi = 0.15$. The injected water temperature is $T_i = 20\,^{\circ}\mathrm{C}$ and the reservoir temperature $T_0 = 86\,^{\circ}\mathrm{C}$. The thermal conductivity $\lambda = 2W/(m \cdot K))$. The specific heat capacity and the density are given by Stoppa et. al as a function of temperature [48].

5.2.2.2 Thermal cooling without conduction

The second model of cooling of a geothermal reservoir due to injection of cold water, is given by the 1-Dimension conservation law which was presented in chapter 3: In the preview chapter we derived an analytical model of the temperature changed in a reservoir due to injection of cold water as:

$$\frac{\partial T}{\partial t} + \frac{\partial G(T)}{\partial x} = 0, \quad T(x,0) = g(x) \tag{5.5}$$

with initial condition

$$g(x) = \begin{cases} T_i & \text{if } x \leq 0 \\ T_0 & \text{if } x \geq 0\ . \end{cases}$$

where $G(T)$ represents the flux function or the energy per unit length and unit time and T is the temperature. Equation (5.5) can be seen as the limit of a convection diffusion equation when conduction is neglected. Since conduction has a smoothening affect on the temperature field, the solution of (5.5) is expected to have sharp jump or discontinuity. The solution of equation (5.5) from the theory of of conservation laws is a shock propagating at a constant speed. The speed of propagation is the rate at witch the cold injected front moves through the reservoir. The solution of (5.5) is :

$$T(x,t) = \begin{cases} T_i & \text{if } x \leq st \\ T_0 & \text{if } x \geq st\ . \end{cases}$$

Equation (5.3) is the solution of an advection diffusion equation where conduction is taken into account, while equation (5.5) models transport phenomenon where conduction is neglected. In (5.5) the smoothening effect represented by conduction is neglected, as a result we will observe a jump or discontinuity in the temperature field as seen in Figure 5.15.

5.2.2.3 Application of thermal cooling with and without conduction to Munadarnes geothermal system

Equation (5.3) represents the solution of a model where heat conduction is the main source of heat transfer. The solution $T(x,t)$, given by Figure 5.14 is expressed in terms of reservoir temperature, injected fluid temperature, injection rate, production rate and heat conduction coefficient. The velocity of the fluid in not present in this model, therefore the model does not take into account convective heat transfer or transport phenomenon. Since

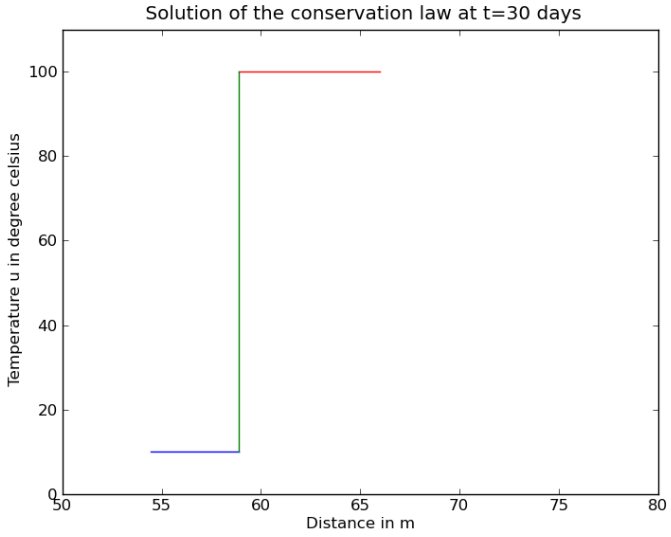

Figure 5.15: Solution of 5.5 at t = 30 days. The reservoir temperature is at $100\,^{\circ}\mathrm{C}$ while the injected water is at $10\,^{\circ}\mathrm{C}$. The heat capacity and density of rock and water are temperature dependent.

heat conduction is predominant, the temperature field is smooth because heat conduction has a smoothing effect on the temperature field. In contrast, equation (5.5) models convective heat transfer. In this model conduction is neglected. In absence of conduction which has a smoothing effect on the temperature field, the temperature profile represented by the solution of equation (5.5) is a discontinuity given by Figure 5.15. The two models are complementary. The intersection of the solutions of the two models gives the production well temperature for a given time t, as shown in Figures 5.16 and 5.17.

In addition, the model given by (5.5) predicts the thermal breakthrough time, that is the time at witch the cold front will reach a production well. The model given by (5.3) predicts the temperature field of the production well when cold water is injected. A shorter thermal breakthrough time will be associated with a rapid cooling of he reservoir, while a longer breakthrough time is acceptable since the cold injected fluid will reach thermodynamic equilibrium along the way.

As an illustration, assume that the distance between the production well and the injection well is $d = 2km$. The production fluid temperature at Munardanes is about $T_0 = 80\,^{\circ}\mathrm{C}$ and a fluid of $T_i = 20\,^{\circ}\mathrm{C}$ is being injected at a rate of $q = 5l/s$ and the production rate is $Q = 8.2l/s$. Assuming a one dimensional channel with $h = 40\ m$, $b = 27m$ and porosity $\phi = 0.15$ and thermal conductivity $\lambda = 2W/(m \cdot K)$). The specific heat capacity and the density are given by Stoppa et. al as a function of temperature [48]. Equation (5.5) predicts the thermal breakthrough time as :

$$t_d = \frac{d}{V_i} \tag{5.6}$$

here d is the distance between the injection well and the production well, and $V_i (i = 1, 2, 3)$ is the thermal front velocity given by Bodvarsson, Stopa and Wajnarowski and the Riemann method, respectively:

$$V_1 = \left(\frac{u_w}{\phi} \frac{\phi \rho_w c_w}{(1-\phi)\rho_r c_r + \phi \rho_w c_w} \right) \tag{5.7}$$

$$V_2 = \frac{u_w}{\phi} \left(\frac{\int_{u_l}^{u_r} U(u)F(u)\mathrm{d}u}{\int_{u_l}^{u_r} U(u)\mathrm{d}u} \right) \tag{5.8}$$

$$V_3 = \frac{1}{(u_r - u_l)} \left(\int_{u_l}^{u_r} \frac{u_w}{\phi} F(u)\mathrm{d}u \right) \tag{5.9}$$

where

$$F(u) = \frac{\phi \rho_w(u) \left(\frac{\partial (c_w(u)u)}{\partial u} \right)}{(1-\phi) \left(\frac{\partial (\rho_r(u)c_r(u)u)}{\partial u} \right) + \phi \rho_w(u) \left(\frac{\partial (c_w(u)u)}{\partial u} \right)}$$

Table 5.3 gives the numerical values of the thermal front velocity for the different models and corresponding arrival time of the thermal front for an injection well located at 2 Km

Table 5.3: Comparison of thermal front velocity of Bodvarsson, Stopa and Wajnarowski and Riemann method, with $\phi = 0.15$, $u_w = 10^{-4} m/s$. Reservoir temperature is $80\,^{\circ}\mathrm{C}$, injected fluid temperature is 20 $20\,^{\circ}\mathrm{C}$. Density and heat capacity for Bodvarsson method, are computed at $80\,^{\circ}\mathrm{C}$.

	Distance (Km)	Thermal front velocity (m/s)	Time (Months)
V_1	2	1.594×10^{-4}	5
V_2	2	2.271×10^{-5}	33.54
V_3	2	2.269×10^{-5}	33.51

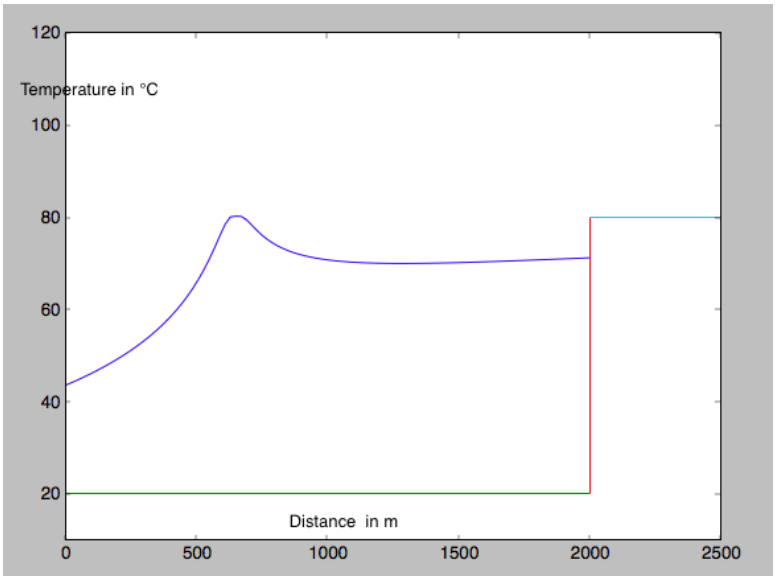

Figure 5.16: Production fluid temperature (top left) and thermal front (right) after 2 years 9 months. Production rate is $8l/s$ and injection rate is $5l/s$. Production well and injection wells are separated by 2 km. With $h = 40m$, $b = 27\ m$ and porosity $\phi = 0.15$. The thermal conductivity $\lambda = 2W/(m \cdot K)$. The vertical axe represents temperature in $^{\circ}\mathrm{C}$ and the horizontal axe represents distance in m

from the Munadarnes production well $MN08$. For the Bodvarsson model, the thermal front velocity is about six time faster then the model from Stopa and Wajnarowski and the Riemann model. For the Bodvarsson model it will take about 4 months for the thermal front to reach the production well, while for the other two models it takes about 33 months for the thermal front to reach the production well. The temperature independent model from Bodvarsson can therefore be seen as the worst case scenario. In Figure 5.16 the discontinuous graph for the Riemann method (right) represents the solution of equation (5.5). The position of the discontinuity between the injected temperature and the reservoir temperature represents the position of the cold front. Here after 2 years and 9 months the cold front will reach the production well located at 2 km from the injection well. Knowing the thermal breakthrough time and the distance between the production well and the injection well we can find the temperature of the production well from (5.3) which is given by $T_0 = 71\,^{\circ}\mathrm{C}$. The smooth graph (top left) represents the evolution of the temperature filed given by (5.3) at $t = 2$ years and 9 months when the production and injection wells are 2 km apart.

Figure 5.17 represents the production zone temperature profile and the position of the cold front after 10 years at a constant rate during that period. By then the cold front has been heated significantly by the hot rock in the reservoir and reached equilibrium. The thermal front has then left the reservoir. The reservoir temperature is $T_0 = 80\,^{\circ}\mathrm{C}$ the same as the initial reservoir temperature before injection. As we move away at about 5 km from the production well, the temperature decrease very slowly to reach $T_0 = 79.3\,^{\circ}\mathrm{C}$ at the location of the cold front.

To recapitulate this section: equation (5.3) describes the temperature distribution of the reservoir by taking into account conduction which has a smoothing effect on the temperature field as indicated by Figure 5.16 and 5.17. Equation (5.3) should be used to predict the temperature of the production well during injection. On the other hand, equation (5.5) ignores conduction. It only considers the propagation of the injected cold front. It should

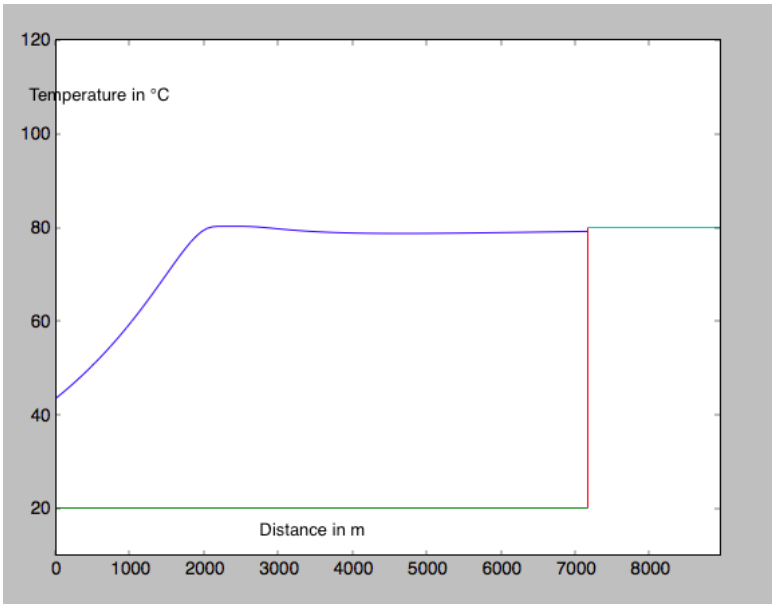

Figure 5.17: Production fluid temperature (top left) and thermal front (right) after 10 years. Production rate is $8l/s$ and injection rate is $5l/s$. With $h = 40\ m$, $b = 27\ m$ and porosity $\phi = 0.15$. The thermal conductivity $\lambda = 2W/(m \cdot K)$). The vertical axe represents temperature in $^{\circ}\mathrm{C}$ and the horizontal axe represents distance in m

Table 5.4: Temperature and pressure response of the reservoir from injection of cold water. $h = 40m$, $b = 27m$, $\phi = 0.15$, $\lambda = 2W/(m \cdot K)$, p($kg/m.s^2$), T($^\circ$C). Production rate is $8l/s$ and injection rate is $5l/s$.

$d(Km)$	T_i	T_r	T_p	$v_{TF}(10^{-5}m/s)$	$t(years)$	P(no injection)	P(injection)
1	20	80	40.9	2.271	20	50	70
1.5	20	80	46.5	2.271	20	50	70
1.9	20	80	52	2.271	20	50	70
2	20	80	74	2.271	20	50	70

not be used to predict the temperature field of the production well. In table 5.4, d is the distance between injection well and production well. T_i is the temperature of the injected water. T_r and T_p are the temperature of the reservoir and the production well respectively. v_{TF} is the rate at which the cold water advances through the reservoir, t is the injection time and P is the pressure in the production well. The temperature of the production well decreases with decreasing distance between injection well and production well. In contrast the pressure significantly increases when cold water is injected into the reservoir. For optimum temperature in the production well the injection well should be placed at a distance of about $2Km$ from the production well.

The main goals of reinjection can be summarise as follows [2]:
1) Counteract pressure decline due to production
2) Maximise the reservoir efficiency by increasing the heat production over the life time of the reservoir
3)Environmental protection scheme
If the purpose is option 3, injection wells can be placed outside the main production field without any direct hydrological connection [2]. If the purpose of the reinjection scheme is option 1 and 2, the rejection wells must be located inside the main production reservoir, in between production wells or on the outskirts of the reservoir but still in direct hydrological connection [2].

From lumped parameter simulation, the munardanes reservoir is unconfined with size about $10.5km^2$. The permeability was estimated to be $70mDarcy$. If injection was carried out in well $MN08$ in Munardanes at a rate of $5l/s$ for a production rate of $8l/s$, it would take 2 years 7 months for the cold front to reach an injection well located at 2 km from the production well. Assuming that the Munardanes production well temperature is at $80\,^\circ$C and the injected energy depleted water is at $20\,^\circ$C, the temperature of the production well after 2 years 7 months of injection would be $74\,^\circ$C. If the production well and the injection well were separated by 1 km, it would take 1 year 4 months for the cold injected front to reach the production well. The temperature of the production well would then be $41\,^\circ$C. The pressure would increase from 20 $kg/m.s^2$ to 70 $kg/m.s^2$ with reinjection.

Chapter 6

Conclusion and future work

This thesis was set out to present various modelling methods in geothermal engineering. A particular focus was set on analytical modelling methods, which are simple, cost effective and do not require large amount of time nor data to provide satisfactory results. These analytical methods have been applied to model various geothermal reservoirs around the world. Their simplicity however comes with a cost: analytical methods can not provide detail and thorough understanding of a geothermal reservoir alone.

The first analytical method models the temperature field of a geothermal reservoir subjected to cold water inflow during reinjection. The model can in theory deal with any type of cold water inflow including cold inflow of ground water at the boundary of the reservoir. The model consists of a first order partial differential equation modelling transport processes. These type of equations are called hyperbolic conservation laws because the quantity being modelled, here temperature front, is conserved from conservation principles. The unique solution is represented as a shock, a steep temperature profile. The steepness of the temperature front is the consequence of the assumption that conduction is neglected. Conduction has a smoothing or damping effect on the temperature field. The main finding is the derivation of the rate at which the cold temperature front propagates. The model proposed by Bodvarsson deals with temperature independent fluid and rock properties. The latter was extended to temperature dependent fluid and rock properties and uses the Characteristics method and conservation of energy to compute the thermal front velocity. The new method called the Riemann method used the theory of hyperbolic conservation laws to derive the thermal front velocity which is the rate at which the cold front moves in the geothermal system. This propagation speed is derived from the well known Rankine-Hugoniot shock condition, derived from the theory of hyperbolic conservation laws. Theoretically, given the injected water temperature and the reservoir temperature, one can compute the velocity of the energy depleted injected fluid, and predict the time at which the cold injected fluid reaches the production well. This velocity depends on the thermal and hydrological properties of the reservoir. The thermal front velocity computed in this thesis is in good agreement with the one computed in the literature from Stopa and wajnarowski. The model proposed by Bodvarsson predicts a thermal front velocity six time larger than the one derived by Stopa and Wajnarowski and the Riemann method. The corresponding thermal breakthrough time from bodvarsson model is six time smaller then the latter models. The Riemann method can easily be extended to 2 and 3 dimensions and rely on the well treated hyperbolic conservation laws in higher dimensions. In this case the energy flux is a vector quantity with three components. The limitation however of this work is the one dimension treatment, which only takes into account the horizontal component of the velocity. Nevertheless, as far as we

know, multidimensional models of thermal front velocity have not been given any attention in the literature.

The second model used in this thesis is a lumped parameter model of a geothermal well located in west Iceland. Lumped parameter modelling can be view as a semi analytical method. The pressure response of the reservoir is given by an analytical formula. The latter contains thermal and hydrological parameters of the reservoir. These parameters are evaluated by simulating pressure or water level data. The software LUMPFIT was used to simulate water level data from well MN08 in Munadarnes. The Simulation revealed that the Munadarnes reservoir is confine and covers an estimated area of $10.5\ km^2$ compared with the Borgarfjordur thermal region which covers an estimated $300KM^2$, with an upflow zone of $100Km^2$ [28, 36]. The permeability of the reservoir intersected by well $MN08$ in Munadarnes was estimated at $70\ m$Darcy based on a 900 m depth. Water level did not change significantly with low production rate. However the water level decreases with increasing production rate. The reservoir pressure and water level are significantly improved by injected water back to the reservoir. To mitigate loss of efficiency in energy extraction because of the cold nature of injected fluid, injection wells can be placed far away from the reservoir, but closed enough to the production wells. The study reveals that injection well can be placed at about $2\ km$ from the production well. At this distance, the production well temperature decreases from $80\,^{\circ}\mathrm{C}$ to $74\,^{\circ}\mathrm{C}$ over a period of 2 years 7 months, with injection rate of $5l/s$ and production rate of $8l/s$. The thermal breakthrough time is based on the Riemann model which gives similar result as the one computed from Stopa and Wajnarowski.

The study was limited to low temperature geothermal systems. It can therefore be extended to include high temperature geothermal systems. The analytical models describing the thermal front velocity can include conduction and the model can be extended to 2 and 3 dimensions, and include multiple injection and production wells. Due to the complexity of the latter model, numerical methods can be used to derive the temperature field and the thermal front velocity. Because of the availability of free open source Computational Fluid Dynamics (CFD) software, the solution of the latter model can be derive with a CFD software such as OpenFoam. The thermal front velocity models used in this thesis assume that 100% of the injected energy depleted fluid reaches the production well. In reality only a fraction of the injected fluid reaches the production well. It is therefore recommended to use a tracer test in practical reinjection operation.

Bibliography

[1] Axelsson, G. “Hydrology and thermomechanics of liquid-dominated hydrothermal systems in Iceland”. PhD Dissertation. Oregon State University, 1985.

[2] Axelsson, G. “Importence of reinjection in geothermal system”. In: *Proceedings of the Workshop for decision makers on direct use of geothermal resources in Asia, United Nation University*. 2008.

[3] Axelsson, G. “Management of Geothermal Resources”. In: *Proceedings of the Workshop for decision makers on direct use of geothermal resources in Asia, United Nation University*. 2008.

[4] Axelsson, G. “Production capacity of geothermal systems”. In: *Proceedings of the Workshop for decision makers on direct use of geothermal resources in Asia, United Nation University*. 2008.

[5] Axelsson, G. “Simulation of pressure response data from geothermal reservoir by lumped parameter model”. In: *Proceedings, Fourteenth workshop on geothermal reseevoir engineering. Standford*. 1989.

[6] Axelsson, G and Bjornsson, G. “Raliability of Lumped Parameter Modeling of Pressure Changes in Geothermal reservoir”. In: *Proceedings of the World Geothermal Congress. Turkey*. 2005.

[7] Axelsson, G, Bjornsson, G, and Montalvo, F. “Quatitative interpretation of tracer test and data”. In: *Proceedings of the World Geothermal Congres. Antalya, Turkeys*. 2005.

[8] Axelsson, G and E, Gunnlaugsson. “Long term Monitoring of High and Low Enthalpy Field Under Exploitation”. In: *Proceedings of the International Geothermal Association, World Geothermal congress,Kokonoe, Kyushu District, Japan*. 2000.

[9] Axelsson, G et al. “Analysis of tracer test data, and injection-induced cooling, in the Laugaland geothermal field, N-Iceland”. In: *Geotermics* 30.6 (2001), pp. 697–725.

[10] Axelsson, G et al. “Sustainable Management of Geothermal Resources and Utilization for 100-300 years”. In: *Proceedings of the World Geothermal Congres. Antalya, Turkeys*. 2005.

[11] Barker, B J, Koenig, B A, and Stack, M A. “Water injection management for resource maximisation: Obserservation from 25 years at the Geysers, California”. In: *Proceedings of the World Geothermal Congress. Florence, Italy*. 1995.

[12] Bear, J. *Dynamics of fluids in porous media*. New York: Elsvier, 1988.

[13] Beretta, G P. *World energy consumption and resources: An outlook for the rest of the century*. Tech. rep. Universita di Brescia. Italy.

[14] Bilicki, Z, Kestin, J, and Michaelides, E E. *Flow in geothermal wells: Part 3 Calculation Model for Self-flowing Well*. Tech. rep. Brown University, 1981.

[15] Bjornsson, G. “A multi-feed zone Geothermal Wellbore Simulator”. Masters Thesis. University of California, USA, 1987.

[16] Bodvarsson, G. “Direct interpretation methods in applied geophysics”. In: *Geoexploration* 4 (1966), pp. 113–138.

[17] Bodvarsson, G. “Thermal problem in sitting of reinjection wells”. In: *Geothermics* 1 (1972), pp. 63–66.

[18] Bodvarsson, G and whiterspoon, P A. “Geothermal reservoir engineering”. In: *Geotherm. Sci and Tech* 21 (1989), pp. 1–69.

[19] Bright, W E and Neri, G. “Depletion Model for the Gabbro Zone Northen part of the Larderello Field”. In: *Proceedings of Second DOE-ENEL Workshop Cooperative Research Geothermal Energy, Berkley, CA*. 1980.

[20] Bringedal, C. “Linear and nonlinear convection in porous media between coaxial cylinder”. Masters Thesis. University of Bergen, 2011.

[21] Bu, X, Weibib, Ma, and Huashan, Li. “Geothermal Energy Production Utilising Abandoned Oil and Gas Wells”. In: *Renewable Energy* 41 (2012), pp. 80–85.

[22] Capetti, G et al. “Fifteen years of injection in the Larderello-Valle Secolo area:Analysis of the production data”. In: *Proceedings of the World Geothermal Congress, Florence, Italy*. 1995.

[23] Cheng, W L, Li, T T, and Wang, C L. “Studies on geothermal power generation using abandoned oil wells”. In: *Energy* 59 (2013), pp. 248–254.

[24] Donaldsson, M Grant I G. *Geothermal Reservoir Engineering*. Academic press, New York-USA: Cambridge University press, 1982.

[25] Edwards, A L. *Trump: A computer program for transient and steady state temperature distribution in multi dimensional systems*. Tech. rep. Report UCRL-14754. Rev. 3. Lawrence Livermore National Laboratory. Livermore CA. USA.

[26] Fowler, C M. *The solid earth: An Introduction to global geophysics*. Cambridge: Cambridge University press, 2005.

[27] Freeze, R A. “Henry Darcy and the Fountains of Dijon”. In: *GROUND WATER* 32.1 (1994).

[28] Georgsson, L S, Johannesson, H, and TBjarnarson. “Geothermal Activity in Borgarfjordur W- Iceland, and the Exploration, Development and Utilisation of the Varmaland/Laugaland geothermal Field”. In: *World Geothermal Congress, Bali, Indonesia*. 2010.

[29] Gould, T L. “Vertical Two-Phase Steam-Water Flow in Gethermal Wells”. In: *Journal of Petroleum Technology* 26 (1974), pp. 833–842.

[30] Gudmudsson, J S and Olsen, G. “Water-influx modelling of the Svartsengi Geothermal field Iceland”. In: *Reservoir Engineering* (1987), pp. 77–84.

[31] Gudmudsson, J S, Olsen, G, and Thorhalsson, S. “Svartsengi Field Production and Depletion Analysis”. In: *Proceedings of Tenth Workshop on Geothermal Reservoir Engineering, Stanford University, Stanford, California*. 1985.

[32] Gudmundsdottir, H. “A Coupled Wellbore-Reservoir Simulation utilising Measure Wellhead Conditions”. Masters Thesis. University of Iceland, Iceland, 2012.

[33] Hagdu, T, Zimmerman, R W, and Bodvarsson, G. "Coupled Reservoir-Wellbore Simulation of Geothermal Reservoir Behavior". In: *Geothermics* 24.2 (1995), pp. 145–166.

[34] Holden, H and Risebro, H H. *Front tracking for Hyperbolic Conservation Laws*. Second. Springer, Berlin. New York-USA: Cambridge University press, 2007.

[35] Kjaran, S P et al. "Reservoir engineering aspects of Svartsengi geothermal area". In: *Geoth. Ressources Concil Trans* 3 (1979), pp. 337–339.

[36] Kristmannsdottir, H et al. "The Reykholt and Husafell Geothermal fields in Borgarfjordura Geochemical study". In: *World Geothermal Congress, Antalya, Turkey*. 2005.

[37] Logg, A. *Injection at the Beowa geothermal reservoir*. Ed. by USA Elsvier. 2011.

[38] Miller, C W. *Wellbore Users Manual*. Tech. rep. Berkley University of California. Report , No LBL-10910, USA.

[39] Norton, T N Narasimhan D L. "Theory of Hydrothermal systems". In: *Ann. Rev. Earth Planet. Sci* 12 (1984), pp. 155–77.

[40] Osullivan, M J, Pruess, K, and Lippman, M J. "State of the art of geothermal reservoir simulation". In: *Geothermics* 30 (2001), pp. 395–429.

[41] Pacheco, P S. *Tracing of injection in the Geysers*. Ed. by USA Elsvier. 2011.

[42] Pritchett, J W. "STAR: A geothermal simulation system". In: *Proceedings of the World Geothermal Congress*. 1995.

[43] Pruess, K. *Mathematical modeling of fluid flow and heat transfer in geothermal systems-An introduction in five lectures*. 2002.

[44] Pruess, K. *THOUGH2 Users Guide*. Tech. rep. Version 2.0 Berkley, University of California, USA.

[45] Saemundsson, A Hjartarson G Bjornsson K. *Stimulation and measurement in well MN 8 in Munadarnes*. Tech. rep. A report prepared for Orkuveita Reykjavik by Iceland geosurvey.

[46] Sayantan, G and Kumar, M. "eothermal Reservoir- A brief Review". In: *Journal of Geological Society of India* 79 (2012), pp. 582–602.

[47] Sorey, L J Fradkin M L and McNabb, A. "On identification and validation of some geothermal models". In: *Water Resour. Res* 17 (1981), pp. 929–936.

[48] Stapo, S and Wajnarowski, P. "Analytical model of cold water front movement in a geothermal reservoir". In: *Geothermics* 35 (2006), pp. 59–69.

[49] Stark, M A et al. "The Santa Rosa-Geyser Recharge Project". In: *Geyser Geothermal Field California, Proceedings of the World Geothermal Congress 2005, Antalya, Turkey, April, 9 pp*. 2005.

[50] Stefansson, V. "Geothermal Reservoir- A brief Review". In: *Geothermics* 26 (2012), pp. 99–130.

[51] Vinsome, P K and Shook, G M. "Multi-Purpose Simulation". In: *Petrol Science and Engineering* 9.1 (1992), pp. 29–38.

[52] Whiting, R L and Ramey, H J. "Application of Material and Energy Balances to Geothermal Steam production". In: *J.Pet.Tech.* (1989), pp. 893–900.

[53] Witherspoon, T N Narasimhan P A. "An integral finite difference method for analysing fluid flow in porous media". In: *Water Resour. Res* 12 (1976), pp. 57–64.

[54] Woods, J and nobloch, P K. “vaporisation of a liquid moving front moving through a hot rock porous medium”. In: *Advance in computation mathematics* (2007).

[55] www.isor.is. Tech. rep. Iceland Geosurvey.

School of Science and Engineering
Reykjavík University
Menntavegur 1
101 Reykjavík, Iceland
Tel. +354 599 6200
Fax +354 599 6201
www.ru.is